Urban Morphology & Climate Hazards: A Systematic Review of Global Evidence, Gaps and Future Directions

Ritu Yadav[1], Andrea Nascetti[1], Thomas Esch[2], Paolo Gamba[3], Yifang Ban[1*]

1 KTH Royal Institute of Technology, Sweden
2 German Aerospace Center - DLR, Germany
3 University of Pavia, Italy

* yifang@kth.se

Abstract

Urban morphology plays a central role in shaping cities' exposure and vulnerability to climate hazards, yet evidence of its influence remains fragmented across hazard types, urban forms, data sources, analytical approaches, and geographic contexts. This systematic review synthesizes evidence on links between urban morphology and six hazards: urban heat, floods, landslides, air-quality degradation, wildfires, and droughts. We reviewed peer-reviewed studies from 2015–2026, a decade of rapid growth in Earth observation, building-footprint data, and urban climate and hazard modelling. A total of 123 studies were identified and systematically analyzed to assess how 2D and 3D urban form has been used to explain hazard intensity, exposure and impacts. The results reveal a growing but uneven evidence base. Urban heat dominates and uses the widest range of indicators, including imperviousness, building density, height, sky-view factor, canyon geometry, surface albedo, and LCZs. Compact, impervious forms increase heat storage and temperatures, while vegetation and favourable configurations promote cooling. 3D morphology and LCZs help explain neighbourhood-scale thermal intensity, ventilation, shading, diurnal contrasts, and heat impacts.. Flood, wildfire, and drought studies rely mainly on 2D indicators such as imperviousness, density, land cover, and settlement extent, with little vertical structure. Air-quality studies integrate 3D morphology as canyon geometry, building height, and ventilation influence pollutant concentration and dispersion. Landslide studies combine terrain, land-cover, and building indicators to assess susceptibility and exposed assets, but rarely use LCZ typologies.Critical gaps include geographic imbalance, limited representation of Africa, Latin America, the Global South, and small and medium-sized cities, scarce globally consistent 3D morphology, limited temporal depth, weak validation, scale mismatches, and insufficient analysis of compound and cascading hazards. Priority directions include developing open, interoperable 2D/3D morphology–hazard datasets, integrating remote sensing with in situ observations and process-based models, expanding research in under-represented regions, and advancing morphology-aware, multi-hazard urban climate assessments to support resilient planning, adaptation, and risk reduction.

1 Introduction

Climate change is intensifying a range of environmental extremes that increasingly threaten cities. More than half of the global population already lives in cities, and this share is projected to reach 68% by 2050. Rapid urbanization has led to expanded exposure to climate hazards (1; 2), while anthropogenic warming has increased the frequency and intensity of extremes such as heatwaves, floods, and wildfires (3). Many events once considered rare are becoming more common (4). The combination of rapid urban growth, aging infrastructure, and intensifying climatic extremes positions cities as "hotspots" in the global risk landscape (5).

Climate hazards in cities do not arise from climate alone. They result from interactions between large-scale climate processes, local land surface characteristics and the built environment. As cities expand, they modify land surfaces, disrupt wind and heat flows, and reshape hydrological pathways (6). These transformations mean that hazards do not simply occur in cities; they are intensified, redirected or dampened by the structure and geometry of the urban fabric. For example, dense built form with common urban surface materials trap energy and suppresses night-time cooling, making urban centers consistently warmer than surrounding rural areas (7). Similarly, impervious surfaces accelerate runoff and reduce infiltration, concentrating flood risk in low-lying areas even under moderate rainfall (8). These physical connections mean that two cities exposed to the same atmospheric extreme can experience fundamentally different levels of hazard intensity depending on how they are built. More broadly, urban form shapes the fundamental pathways through which hazards intensify and propagate.

Urban morphology, understood as the spatial arrangement and geometric properties of the built environment, is therefore central to climate risk dynamics. Two-dimensional (2D) characteristics such as impervious surface fraction, building footprint density, and land cover composition influence runoff generation, heat storage, and surface atmosphere exchange. Three-dimensional (3D) features, including building height, street canyon geometry, sky view factor, and volumetric density, regulate shading, ventilation, radiative trapping, and pollutant dispersion (9; 10; 11). Across hazards, these morphological metrics have been linked to urban microclimate, hydrological response, thermal exposure, fire spread, and pollutant dispersion, demonstrating that urban form systematically shapes climate hazard dynamics (12; 13).

Over the last decade, satellite-based Earth observation and related remote sensing datasets have become the primary basis for quantifying both urban morphology and climate hazards from city to global scales. A range of approaches has emerged to characterize urban morphology. The Local Climate Zone (LCZ) system provides a globally consistent typology by distinguishing forms such as compact high-rise, open low-rise, or industrial large low-rise areas, each associated with distinct thermal and aerodynamic properties (12). These LCZ maps are typically produced from multispectral and SAR satellite imagery combined with ancillary geospatial data. In parallel, remote sensing building products, digital surface models, and high-resolution 3D building data enable quantitative assessment through 2D/3D building indicators such as density, height and street configuration (14). Together, LCZ classes and 2D/3D building indicators provide complementary ways to incorporate urban morphology into climate-hazard analysis. At the same time, remote sensing provides key information on hazard-relevant variables, ranging from thermal conditions and vegetation structure to land cover, soil moisture and surface deformation, which are often combined with in situ and model-based data within urban climate and hazard analyses.

Despite these advances, research linking climate hazards and urban morphology remains fragmented across the literature. Studies differ widely in spatial scale, hazard focus, modeling approach and the morphological indicators they use. Many studies focus on single hazards or single cities, use inconsistent morphological definitions, or apply coarse land-use proxies that overlook 3D structure. Reviews of disaster risk reduction and urban climate research point to limited cross-city comparability, uneven geographic coverage and insufficient integration of high-resolution morphological data, particularly in rapidly urbanizing regions (15; 16; 17; 18). As a result, it remains difficult to build a coherent global understanding of how urban form influences climate-related risks.

A systematic global review is therefore needed to provide clarity. Such a review consolidates evidence from different hazards, cities and regions and compares how various morphological representations (2D or 3D morphological metrics and LCZ classifications) are used to study climate hazard risks. It highlights where knowledge is well established and where major gaps persist, particularly the role of 3D structure,

morphology–hazard interactions and the disparities in the availability and resolution of urban morphological data across different parts of the world. The objectives are threefold:

1. To systematically review and synthesize global evidence base that examines the relationships between urban morphology and climate-related hazards;
2. To critically assess the use of 2D, 3D morphology representation, including building level indicators and LCZ-based classification across different hazard contexts; and
3. To identify key data, methodological, and geographic gaps and to outline future directions for advancing morphology-aware urban climate research.

The paper proceeds by establishing the conceptual framework for linking urban form and climate hazards (Section 2), followed by a description of the systematic review methodology (Section 3, overview PRISMA 2020 Figure 1). Section 4 contains results synthesize trends between the six climate hazards (urban heat island (UHI), floods, landslides, air quality, wildfires, drought) and morphological representations, comparing data sources, analytical methods and reported morphology-hazard dynamics for each hazard. Section 7 identifies key research gaps in data coverage, spatial resolution, temporal depth and geographic representativeness. Section 8 concludes by outlining priority research directions for advancing morphology-aware, multi-hazard urban climate assessment.

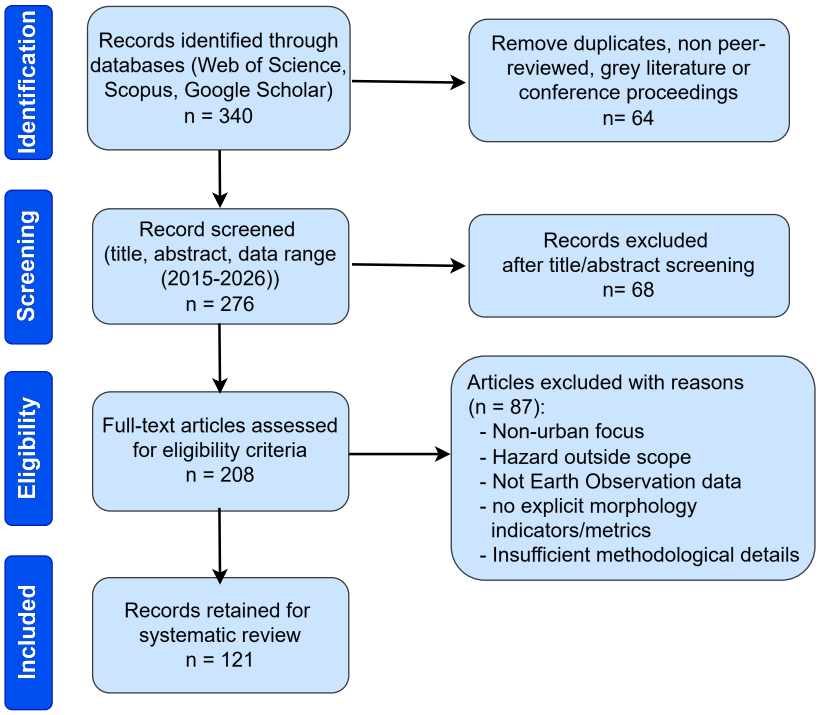

Fig 1. PRISMA 2020 flow diagram for identification, screening and inclusion of relevant urban hazard-morphology literature (19).

2 Conceptual Framing: Linking Urban Morphology and Climate Hazards

Climate hazards in urban environments emerge from interactions among atmospheric processes, land-surface characteristics, built structures and human systems. Urban morphology constitutes a central element within this coupled system, as it governs the transfer of heat, moisture, momentum and pollutants, thereby shaping

both hazard exposure and associated impacts. The framework presented in Figure 2 outlines the key physical pathways through which 2D and 3D urban form influences climate hazards.

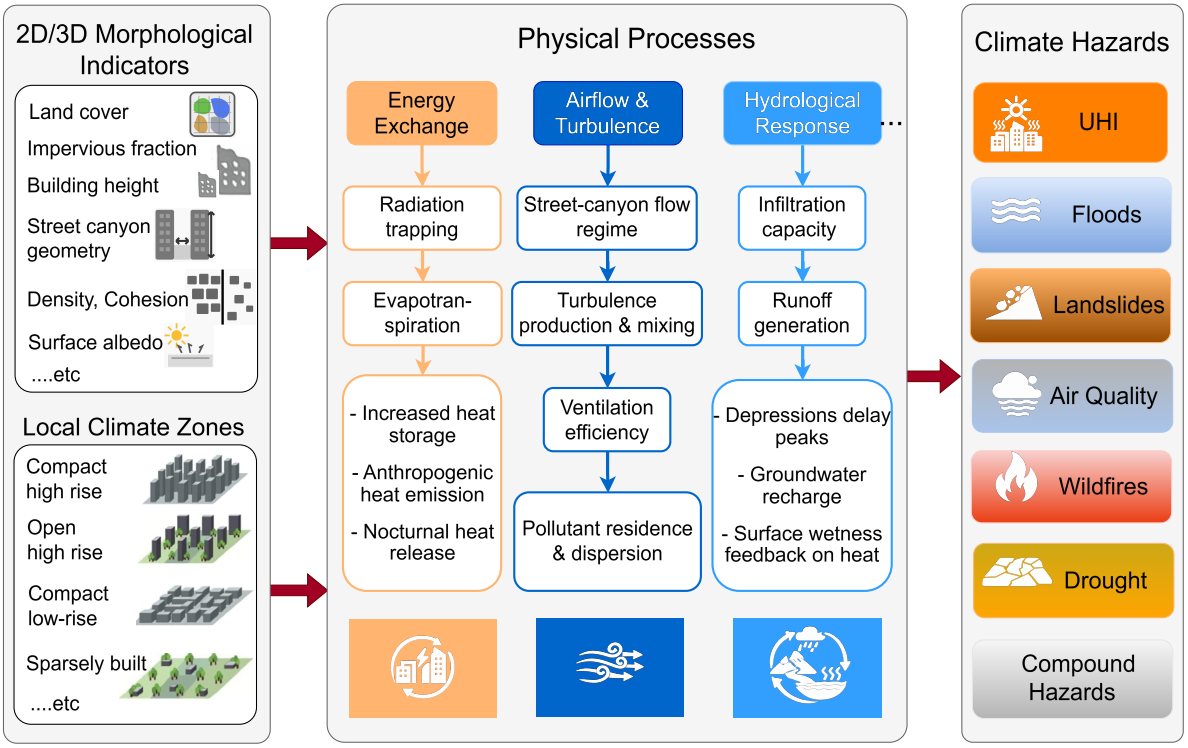

Fig 2. Linking Urban Morphology and Climate Hazards.

Urban surfaces and structures modify the local energy balance. Impervious materials, sparse vegetation and dense street canyons shift the partitioning of solar radiation toward sensible heating while suppressing evapotranspiration, intensifying the urban heat island and altering exposure at neighborhood scales (10; 20; 21). Building geometry influences night-time long wave cooling and can trap heat within narrow canyons, while height contrasts and street orientation shape ventilation pathways that either disperse or accumulate heat and pollutants (22; 23). Hydrological pathways are equally morphology-dependent: 2D patterns of imperviousness, land cover and drainage impact infiltration, runoff generation and the timing of peak flows (8; 24); 3D structure, such as building placement, street geometry, elevation, steers water flow and concentrates pluvial flooding during extreme precipitation (25). The built environment thus governs both the amplification and attenuation of hydrological hazards. Air quality, drought and wildfire risks also respond to physical form. Vegetation fraction and configuration influence evapotranspiration, soil moisture and local cooling, shaping drought sensitivity and heat–drought interactions (26; 27). In fire-prone regions, the continuity of fuels at the urban–rural interface interacts with topography and wind corridors created by urban geometry (28). Pollutant dispersion depends strongly on canyon form: tall, narrow canyons trap pollutants, whereas open or staggered geometries enhance turbulent mixing (29).

These mechanisms collectively demonstrate that urban form mediates, amplifies and spatially redistributes climate hazards. Across all six climate hazards, i.e., heatwaves, drought, air quality degradation, wildfires, floods, landslides and compound hazards, a consistent pattern emerges: that the impact distribution and intensity are not uniform, but rather shaped by the geometry, materials and layout of the built environment.

Most literature studies that build on these physical processes adopt a broadly similar analytical pipeline, combining urban morphology indicators with hazard and auxiliary environmental data to analyze and quantify the morphology-hazard relationships using statistical and modeling methods Figure 3 provides a schematic overview of this literature-wide structure, showing how the conceptual pathways in Figure 2 are translated into measurable indicators and analytical workflows. Together, the physical pathways (Figure 2) and the analytical pipeline (Figure 3) provide the conceptual foundation for this review, which guides how we

identify morphology-related indicators in the literature, classify data sources and methods, and how we interpret reported morphology–hazard relationships across different hazards, spatial scales and world regions.

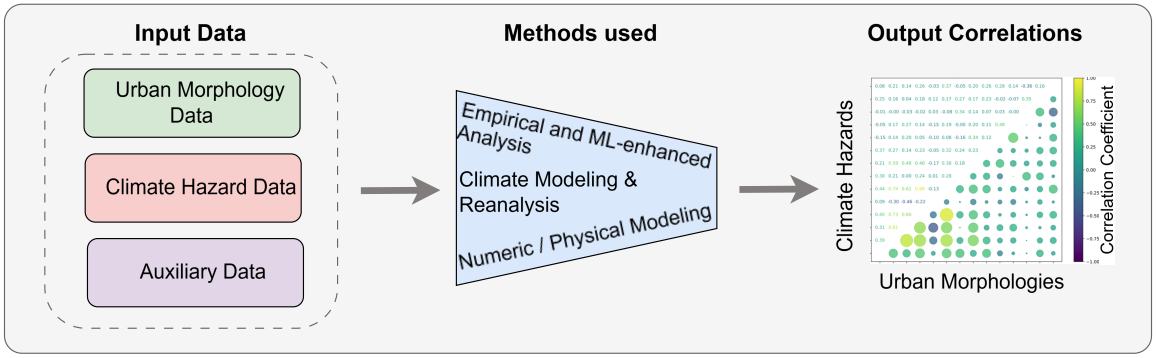

Fig 3. Structure of Urban Morphology and Climate Hazard Studies. Studies typically combine hazard data, urban morphology indicators and auxiliary environmental variables as inputs. These are analyzed using statistical, machine learning or physical modeling approaches, and results are expressed as correlations between urban morphology and specific climate hazards.

3 Methods and Materials

This review systematically examines how urban morphology interacts with climate hazards across a global body of peer-reviewed research. The temporal, thematic and geographic boundaries were defined to capture the rapid methodological evolution of the field while maintaining a connection to early foundational works. The search protocol, eligibility criteria, and data-extraction framework were designed to be transparent and reproducible, following the Preferred Reporting Items for Systematic Reviews and Meta-Analyses (PRISMA 2020) guidelines.

3.1 Scope and Definitions

The review focuses primarily on studies published between 2015 and 2025, reflecting a decade in which urban climate science expanded through widespread availability of high-resolution satellite products, detailed building datasets and improved urban land-surface and climate models.

Hazard Selection

Six climate hazards form the thematic core of this analysis: heatwaves, floods, landslides, air-quality degradation, wildfires, and droughts. These hazards were selected for three reasons:

1. They represent the dominant climate-related threats to cities as identified by the IPCC Fifth and Sixth Assessment Reports, which consistently highlight these hazard types as the most consequential for urban systems due to their impacts on health, infrastructure, water supply, air quality and economic activity (30; 31);

2. These hazards align with the UNDRR Global Risk Assessment Framework, which emphasises them as priority risk drivers in cities and classifies them as core components of global multi-hazard risk profiles (18; 32);

3. Each of these hazards exhibits strong physical and functional linkages with urban morphology e.g., heatwaves with urban heat islands and ventilation, droughts with water demand and surface permeability, air-quality degradation with canyon geometry and dispersion, wildfires with the Wildland Urban Interface (WUI), extreme precipitation with hydrological response, floods with drainage and surface sealing and sea level rise with coastal settlement patterns.

Together, these six hazards cover the major climatic stressors for which morphological characteristics have demonstrable influence.

Urban Morphology

Urban morphology is defined in this review as the spatial, geometric and material configuration of the built environment, encompassing the layout and physical form of buildings, streets, open spaces and vegetation. This definition follows established traditions in urban climatology and urban form research (33; 34). Morphological indicators fall into three broad categories.

1. **2D indicators** (14), such as impervious surface fraction, land cover composition, surface albedo, compactness and vegetation cover, which influence surface–atmosphere exchanges, thermal storage and hydrological responses.
2. **3D indicators** (14), including building height, height variability, volumetric density, sky-view factor, canyon geometry and the geometry of roofs and façades metrics widely used in microclimate and airflow modeling due to advances in lidar, stereo photogrammetry and global building height datasets (14; 35; 36)
3. **LCZ**, a classification-based system, which provides a standardized typology of urban form and surface cover (12). Open LCZ maps are generated worldwide in a consistent way, using a universal typology (17 classes: 10 built, 7 natural) and enabling comparison across cities/regions/countries (see Figure 4). LCZ data represent an evidence-based spatial layer with associations to urban canopy parameters (roughness, imperviousness, etc.), making it relevant for applications related to urban climate, the heat island effect and climate adaptation and modeling.

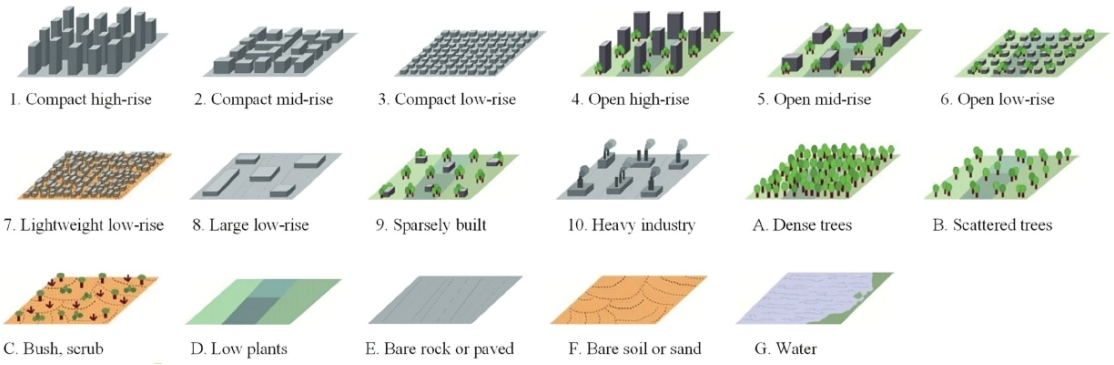

Fig 4. Local Climate Zone Classification. Each of 17 classes (10 built, 7 natural) has a distinctive surface property, such as height/packing, object roughness, or dominant land cover. The physical properties of all zones are measurable and nonspecific as to place or time (12)

The review draws from peer-reviewed journal articles across urban climatology, remote sensing, environmental science, hydrology, atmospheric science and urban planning. The geographical scope is global, without restrictions by region, climate zone or income group. Studies were included when they explicitly linked at least one morphological descriptor to one or more of the six selected hazards. This broad spatial coverage reflects ongoing calls in recent IPCC and UNDRR assessments for wider geographic representation and more consistent multi-hazard evaluation in urban areas.

3.2 Literature Search and Screening

The literature search followed a structured protocol inspired by "Preferred Reporting Items for Systematic Review Recommendations" (PRISMA) guidelines, ensuring transparency and replicability in the identification, screening and selection of studies (19). Three major bibliographic databases formed the core search environment: **Web of Science**, **Scopus** and **Google Scholar**.

The search strategy combined key terms for urban systems, climate hazards and morphological descriptors. The baseline search string was structured in the format: ("urban" OR "city" OR "built environment") AND (hazard-specific terms) AND ("urban morphology" OR "built form" OR "urban form" OR "3D city model" OR "building height" OR "Local Climate Zones" OR "LCZ" OR "street canyon" OR "impervious surface"). Hazard-specific terms were adapted for each of the six hazard classes (e.g., "urban heat island", "floods", "wildfire", "air pollution", "drought", "landslide", "compound hazard"). Searches were conducted in December 2025 and the databases were last accessed on 15 June 2026. No automation or AI-based screening tools were used; all screening was performed manually by human reviewers.

Inclusion Criteria

Studies were included when they:

1. examined at least one of the six selected climate hazards;
2. analyzed cities or urbanized regions;
3. incorporated explicit morphological data through 2D/3D indicators or LCZ classification;
4. provided empirical, modeling or observational evidence; and
5. were published in English between 2015 and 2026, with selected pre-2015 landmark studies included for foundational context.

Exclusion Criteria

Studies were removed when they:

1. relied solely on coarse urban/non-urban proxies;
2. lacked a morphological component;
3. focused exclusively on rural landscapes, or provided insufficient methodological detail.
4. Reviews, theses, conference abstracts and non-technical reports were excluded unless they introduced core datasets or frameworks relevant to the study.

The screening process occurred in two stages. First, all retrieved records were screened at the title and abstract level to remove clearly irrelevant works. Second, full-text screening was conducted for all remaining studies to assess methodological quality, data sources, hazard focus and morphological relevance. Studies meeting all inclusion criteria were retained and coded systematically. Citation chaining was used to identify additional influential works, particularly in underrepresented geographical regions. The workflow in Figure 1 summarizes the screening process. The flow diagram includes:

1. **Identification:** total records retrieved from databases and institutional repositories, with duplicates removed.
2. **Screening:** number of records excluded after title and abstract review.
3. **Eligibility:** full-text records assessed; studies excluded with reasons (e.g., not urban, no morphological data, hazard not covered).
4. **Inclusion:** final set of peer-reviewed articles and high-quality literature included in the review.

Here are some examples of the rejected papers (87) which failed the full text screening under specified eligibility criteria, such as lack of explicit use of urban morphology indicators or methods (37; 38; 39; 40). Each stage of the screening was performed independently by two reviewers, with disagreements resolved through consensus discussion. Where ambiguity persisted, a third reviewer adjudicated. This dual-review approach was applied to both the title/abstract and full-text stages.

3.3 Data Extraction and Study Coding

After the final set of studies was identified, each publication was processed using a structured data-extraction protocol designed to efficiently draw comparisons across diverse hazard types, morphological representations, used data types and used methodologies for analysis. The extraction protocol was developed iteratively, drawing on established environmental review procedures (41) and adapted to the specific needs of urban climate research.

For every study, bibliographic metadata were recorded: first authors, year, journal, study region and hazard category. The substantive coding then captured four broad domains. The substantive coding then captured five broad domains, detailed in Sections 3.3.1 to 3.3.6. All extracted data were compiled into a structured database that supports the hazard-specific and cross-hazard analyses presented in subsequent sections. To enhance consistency, each study was coded independently by two reviewers, with discrepancies resolved through consensus. Ambiguous cases, such as studies with partial morphology integration, were discussed and re-evaluated, following recommended procedures in systematic environmental reviews (42).

3.3.1 Coding of Climate Hazards

Each publication was assigned a primary hazard category corresponding to the dominant climate driver analyzed: heatwaves, droughts, air quality, wildfires, landslides, or floods. This structure aligns with global climate-risk frameworks that treat these hazards as distinct but interrelated stressors in urban environments (31; 43). Studies that examined interacting or cascading events were additionally tagged with compound hazards, enabling recognition of compound processes such as heat–pollution episodes or rainfall-induced landslides. Compound event tagging reflects growing scientific emphasis on multi-hazard interactions (44). This step allows comparison of hazard metrics across studies and supports identification of methodological variability.

3.3.2 Coding of Urban Morphology

Urban morphology was classified using a set of indicators, each corresponding to how built forms were operationalized in the reviewed studies (subsection 3.1): (i) 2D indicators (e.g., planimetric or surface-based metrics); (ii) 3D indicators (e.g., height, volumetric or geometric metrics) and (iii) LCZ-based classifications. These flags were assigned independently, allowing studies to receive multiple codes when using hybrid approaches, for instance, pairing LCZ maps with high-resolution vector-based 2D building indicators for analysing the impact of green structure and grey structure on UHI. This coding approach is consistent with urban climate meta-analyses that treat morphology as a multi-representational domain rather than a single definitional construct (12; 36).

3.3.3 Coding of Hazard Data Sources

We capture metadata describing data sources (satellite, aerial, meteorological), spatial resolution and major processing steps. This information is fundamental for evaluating how climate hazard data quality shape the reported relationships between climate hazards and urban morphology. Overall, we categorize the source data into five major groups:

1. Remote Sensing data: includes optical, thermal, LiDAR and radar observations from aerial or satellites such as Landsat, Sentinel, Terra Aqua, Suomi NPP and GEDI. Based on spatial resolution, remote sensing data are commonly classified into three categories: (i) **coarse resolution** ($>$ 100 m), (ii) **medium resolution** (30–100 m) and (iii) **high resolution** (spatial resolution $<$ 30 m). These sensors and their derived products provide consistent, spatially explicit information on land cover, built-up structure, morphological indicators, surface temperature, vegetation and water dynamics, enabling hazard–morphology analysis across regions and time.

2. **In-situ Measurements:** refer to ground-based observations including meteorological stations, air-quality monitors, hydrological gauges, GNSS sensors and urban flux towers that supply

high-accuracy point data used for model calibration, hazard attribution and validation of remote-sensing outputs.

3. **Models and Reanalysis:** comprise global and regional climate simulations (e.g., CMIP, CORDEX), atmospheric and land-surface reanalysis datasets (ERA5, MERRA-2), hydrological simulation and hazard-specific model outputs such as downscaled precipitation, heatwave indices, or flood inundation layers. These datasets offer physically consistent spatiotemporal fields that extend observational records and describe compound or future hazard conditions.

Together, these categories reflect the multi-source data landscape required to understand how cities interact with a changing climate, particularly as finer-resolution observations and analytic tools continue to expand the possibilities for urban hazard research.

3.3.4 Coding of Urban Morphology Data Sources

We also captured the urban morphology data sources and categorized it into four groups:

1. **Coarse Resolution Remote Sensing**($>$ 100 m): includes morphology derived from coarse resolution landcover, urban fraction or vegitation fraction data from remote sensing sources such as VIIRS, MODIS etc.

2. **Medium Resolution Remote Sensing**(30- 100 m): morphology derived between 30m to 100m spatial resolution such as WUDAPT LCZ, CORINE landcover, building coverage or height products WSF and GHSL.

3. **High Resolution Remote Sensing**($<$ 30 m): morphology derived at less than 30m spatial resolution from remote sensing data such as aerial images, LiDAR data or satellites data from planet, DigitalGlobe and worldview.

4. **Simulation:** include urban morphology derived from simulated urban environments in models such as CFD, ENVI-met, uDALES and WRF.

3.3.5 Coding of Analytical Methods

The analytical approach of each study was documented to characterize the underlying modeling or empirical framework. To enable systematic comparison across the literature, we grouped the methodological strategies into five categories.

1. **Empirical Analysis:** encompasses observational and statistical studies, including land surface temperature, land cover and indicators of built form. These studies commonly apply statistical regression, correlation, clustering or other comparative designs to examine hazard and morphology relationships within or across cities.

2. **Machine Learning Enhanced Empirical Analysis:** includes studies that integrate remote sensing or GIS-based inputs with machine learning models such as Random Forest, XGBoost, neural networks and SHAP interpretation.

3. **Numeric / Physical Modeling:** covers investigations that simulate environmental processes through microclimate models, energy balance and radiation schemes, computational fluid dynamics, or building and neighborhood scale physical representations used to examine ventilation, heat transfer, or flood hydraulics.

4. **Climate and Atmospheric Modeling and Attribution:** refers to research that employs global and regional climate models, reanalysis products, urban canopy schemes and event attribution frameworks to diagnose or project the influence of urban morphology under present or future climate conditions.

3.3.6 Coding of Geography

Each study was assigned to a broad geographical region to capture the spatial distribution of research effort. The regional categories are: Africa, Asia, Europe, Latin America & the Caribbean, North America and two Global categories (i) "global" for analyses using globally consistent datasets focused on aggregate exposure (e.g., drought, sea-level rise), and (ii) "global-scale" for studies analysing multiple sites across the world. This classification provides insight into geographic imbalances in the evidence base, reveals areas where hazard and morphology interactions remain understudied and highlights the extent to which findings may reflect regional climatic or morphological contexts.

3.4 Risk of bias

Three aspects of the review design introduce potential bias in the evidence base. Restricting the search to **English-language peer-reviewed publications** may exclude relevant studies from regions where research is disseminated in national journals, and may introduce publication bias toward studies reporting significant morphology–hazard relationships. The **temporal boundary of 2015–2026**, while justified by the rapid methodological evolution of the field, excludes earlier foundational work that established important morphology–hazard linkages. Limiting sources to **three bibliographic databases** (Web of Science, Scopus, Google Scholar) may have missed studies indexed only in regional or discipline-specific repositories. Together, these choices may skew the distribution of coded data source categories and analytical methods.

4 Morphology-Hazard Relationships: A Decade of Global Evidence (2015-2026)

Despite increasing interest in urban climate risk, the literature explicitly examining the relationship between urban morphology and climate hazards remains limited. To the best of our knowledge, 123 peer-reviewed studies published between 2015 and 2026 directly examine the relationship between climate hazards and urban forms. The evidence base is therefore still relatively narrow and unevenly developed.

4.1 Geographic Distribution of Evidence

The literature is concentrated geographically, with nearly half of the studies from Asia (Figure 5) and within Asia, these studies are concentrated mainly in China. A substantial number of studies also focus on European cities. In contrast, large parts of the world remain sparsely studied, particularly Africa and Latin America, despite their high exposure to climate hazards. Most studies focus on major metropolitan areas and megacities, while small and medium-sized cities are largely underrepresented. Although several studies are conducted at global-scale, spanning multiple cities, only a couple of studies are fully global. Hazard representation is similarly skewed. Urban heat dominates (36%) the literature examining how urban form influences hazard intensity and impacts. In contrast, although floods(14%), landslides (14%), air quality (15%), wildfires (0.09%) and droughts (0.08%) are widely studied in general hazard research, only a limited number of studies explicitly analyze the role of urban morphology in shaping these hazards. Compound hazards are rarely studied. The dominance of heat-morphology research corresponds with greater indicator diversity and methodological experimentation in that domain, whereas the analysis in other hazards is narrowly operationalized.

4.2 Data, Methods and Morphology Indicators across Hazards

Although the reviewed studies examine different hazards and urban contexts, they share a broadly comparable analytical structure (Figure 3). They combine hazard datasets, urban morphology indicators and auxiliary environmental variables and examine these relationships using empirical analysis, machine learning or physical modeling (Table 1). Thus, differences across hazards arise not from fundamentally different research frameworks, but from variation in dominant data and modeling strategies within a shared analytical structure.

Table 1. Overview of input data and analysis method categorizations used in reviewed literature.

	Aspect	Examples	Description
Input Data	Urban Morphology Data	2D/3D building indicators: coverage ratio, floor to area ratio, density, setback, height variation, width to height ratio, volume, canyon aspect ratio	Quantitative descriptors of the horizontal and vertical structure of the built environment derived from remote sensing data such as satellite imagery, LiDAR, and orthophotos
		Local Climate Zone (LCZ) classifications: compact high-rise, compact low-rise, open high-rise, sparsely built, heavy industry etc	A standardized land-use and land-cover classification that groups urban and natural surfaces based on morphological, thermal, and surface-cover properties. Also derived from remote sensing data such as satellite imagery, LiDAR, and orthophotos
	Hazard Data	Flood extent maps, heatwave occurrence maps, air-quality records, wildfire maps, landslide maps	Spatial or point-based representations of hazard occurrence derived from remote sensing data, in-situ measurements or simulated using different software
	Auxiliary Data	road networks, DEM, topography, rainfall, wind speed, humidity, soil properties, population data	Supporting environmental, infrastructural, and socio-demographic datasets derived from in-situ measurements, cadastral datasets, and administrative records
Method	Empirical and ML-enhanced Analysis	regression, correlation, clustering, random forest, XGBoost, SHAP interpretation	statistical and machine-learning-based analyses used to explore relationships between hazards and urban morphology
	Climate Modeling and Reanalysis	climate-driven flood risk projections; urban heat amplification under climate change; reanalysis-based air-quality and meteorological forcing datasets	studies employing global and regional climate models and reanalysis products to diagnose long-term climate variability, trends, and scenario-based projections influencing hazard occurrence under present and future climate conditions
	Numeric / Physical Modeling	slope-stability models for landslides; hydrodynamic flood models; urban energy-balance models for UHI; numerical dispersion and chemistry models for air-quality degradation	Process-based simulations that explicitly resolve physical mechanisms governing hazard dynamics using mass, momentum, and energy conservation equations, typically at local to neighborhood scales

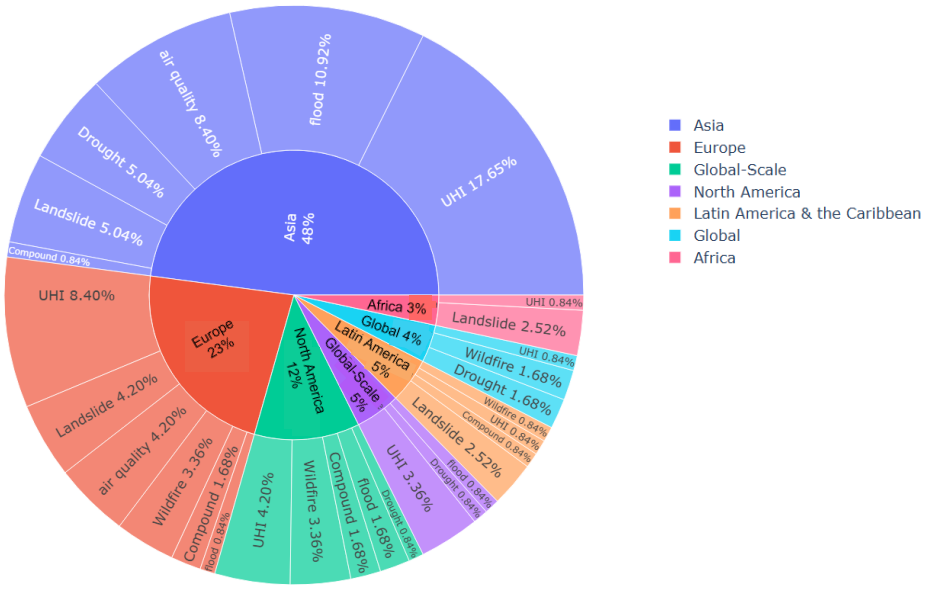

Fig 5. Distribution of Urban Morphology - Hazard Studies: Asia accounts for the largest share of studies (48%), but this dominance is driven by research conducted in China. In contrast, rapidly urbanizing regions in Africa (3%) and Latin America and the Caribbean (5%) remain sparsely represented. Note: While global analysis are on globally consistent data, global-scale studies only span multiple cities across the globe.

4.2.1 Urban Morphology Data Sources

Across the 121 reviewed studies, remote sensing data constitute the primary source for deriving urban morphology, with a fraction of studies (26/121) relying on simulated urban environments. Figure 6 maps data type categories onto morphological representation outputs across the evidence base, showing that medium-resolution remote sensing is the most widely used input (50 studies). In terms of morphological output, 2D indicators dominate (57 studies), followed by combined 2D & 3D representations (40 studies), LCZ classifications (26 studies) and purely 3D indicators (3 studies).

2D morphological indicators are derived from remote sensing data spanning a wide resolution range, from coarse global settlement layers providing impervious surface fraction and built-up extent at 100m–1km (45; 46), through medium-resolution 30–100m products for land-cover composition and building coverage ratio (47; 48; 49; 50), down to high-resolution raster or building footprint vector datasets (Microsoft Global Building Footprints) and locally derived aerial or LiDAR-based footprints at sub-metre accuracy (51; 52; 53). Purely 3D representations remain rare (3 studies), relying on simulation environments CFD and WRF or high-resolution LOD building models (54; 55). Combined 2D & 3D representations are more common (40 studies) and typically use simulation environments such as CFD or microclimate models (ENVI-Met, WRF), medium-resolution raster products or high-resolution vector footprints or LOD building models to simultaneously capture horizontal extent and vertical structure (56; 57; 58; 59).

LCZ classifications (26 studies) are predominantly derived at 100 m resolution through the WUDAPT framework (60; 61; 62). This globally consistent representation bridges fine-scale morphological detail and broad spatial coverage, making it tractable to link urban form type to hazard outcomes at city scale. However, its principal limitation is internal heterogeneity: areas sharing the same LCZ class can vary substantially in actual building configuration, potentially obscuring neighbourhood-scale differences in hazard exposure.

4.2.2 Hazard Data Sources

Our review shows that hazard data regimes differ systematically across domains (see Figure 7). The evidence base draws on a diverse mix of observational and model-simulated datasets, with each hazard displaying its

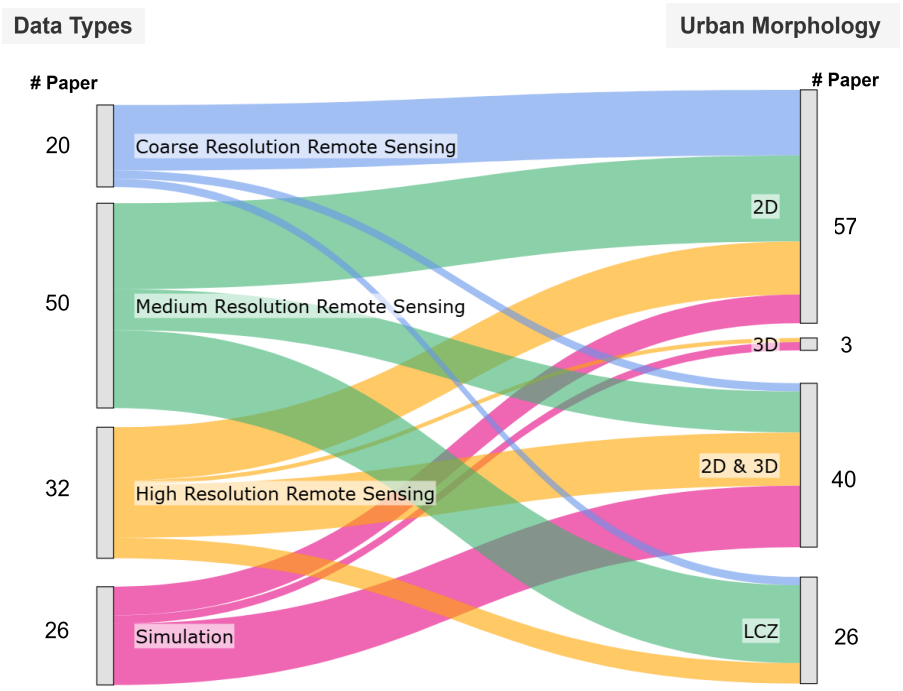

Fig 6. Types of Data Sources Used to derive Urban Morphology. Analysis of the evidence base shows that remote sensing data is the main source for urban morphology derivation. Remote sensing data is further categorized into coarse (>100 m), medium (30-100 m) and high (<30 m) resolution remote sensing data. Also, the literature is heavily dependent on 2D indicators.

own characteristic data profile. Urban heat and wildfire studies are largely dominated by remote sensing, reflecting the direct observability of surface temperature and burn extent from satellite data. Floods and landslides are primarily model-driven with remote sensing providing essential inputs and validation such as topography, land cover, soil moisture and deformation signals (63; 64; 65; 66; 67). Flood research depends heavily on hydrodynamic simulations such as TELEMAC (52; 68), while landslide studies rely on slope-stability and susceptibility models (e.g., CHASM, FSLAM)(69; 70). Drought studies use coarse remote sensing data and simulations (71; 72). Similarly, air-quality studies more commonly use in-situ monitoring networks alongside atmospheric transport and dispersion models such as CFD, ENVI-met, and TREM (73; 74; 75).

Urban heat stress research has a strong reliance on satellite-based land surface temperature (LST) with a multi-resolution data framework, with medium and coarse resolution satellite thermal products forming the primary data used in the evidence base. The UHI intensity is mainly derived from Landsat 8 (30 m), VIIRS (375 m–1 km), MODIS (1 km) and ERA5-HEAT (31 km). While most studies examine daytime or daily average conditions, only a few investigations incorporate nighttime observations, particularly using MODIS Terra nighttime (1 km) and SDGSAT-1 (30m) LST products (61; 76; 77). Additional UHI analyses use climate and microclimate simulation models such as CMIP, ENVI-Met, uDALES and WRF simulations, which allow manipulation of thermodynamic parameters and urban forms to assess UHI-morphology relationships across scales (56; 78). Some studies integrate in-situ air-temperature measurements using sensors such as the HOBO U23X-00188.

For urban flood studies, LiDAR-derived DEMs serve as the primary dataset, providing the detailed elevation and slope needed to model overland flow, ponding, drainage pathways and identifying low-lying plains (25; 79). The medium resolution SRTM 30 m or ASTER 30 m DEMs are used when LiDAR coverage is unavailable (51; 55). Flood propagation is most commonly (47.62%) simulated with 1D/2D hydraulic models such as HEC-RAS, LISFLOOD-FP and TELEMAC-2D, which depend on supporting datasets including GIS-based drainage networks and road networks and in-situ rainfall records (52; 80). Overall, flood

studies rely strongly on high-resolution DEM and hydrodynamic modeling with in-situ hydrological observations (rainfall, gauge records and streamflow).

Landslide and urban morphology studies rely on an integrated dataset framework combining high resolution terrain information, land-cover and vegetation maps, rainfall and climate inputs and slope-stability modeling tools. Terrain representation is commonly derived from LiDAR or orthophoto-based DEMs (1–5 m), TanDEM-X/ALOS DSMs (58; 70) and medium-resolution SRTM or ASTER DEMs (30–90 m), which support calculation of slope, curvature, TWI and other topographic predictors (81; 82). Landslide inventories play a central role and are typically mapped from high-resolution imagery (Planet, Google Earth, WorldView) or medium-resolution satellites (Landsat, Sentinel-1/2) (57; 83). Many studies further model landslide susceptibility and failure processes using mechanistic tools such as CHASM, FSLAM, supported by hydrological and land-surface simulations (70; 84). Rainfall forcing is drawn from GPM and GPCC precipitation datasets, ERA5 reanalysis, national meteorological networks and regional climate models (83; 85)

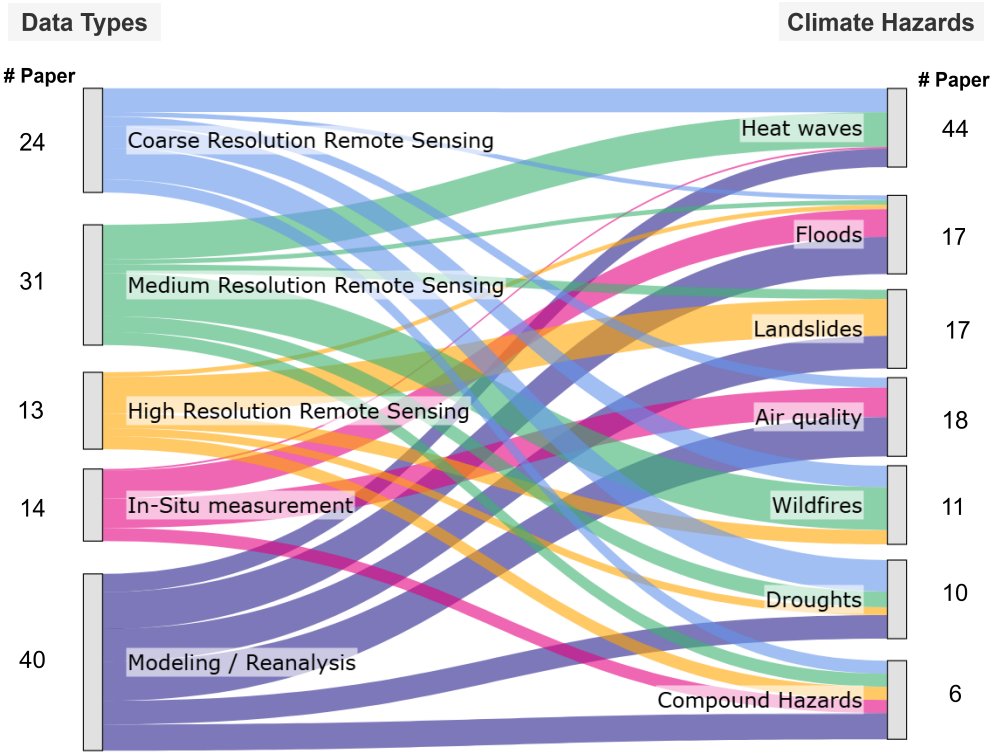

Fig 7. Types of Data Sources Used Across Climate Hazards. Analysis of the evidence base shows that remote sensing data dominate heat wave, wildfire and compound hazard studies. In contrast, floods, landslides and air quality hazard data primarily come from model simulations and in situ measurements. Remote sensing data is further categorized into coarse (>100 m), medium (30-100 m) and high (<30 m) resolution remote sensing data. Also, literature is heavily skewed toward heat waves, with minimal focus on compound hazards.

Air quality studies, by contrast, depend more heavily on ground-based monitoring networks, which remain essential for measuring $PM_{2.5}$, PM_{10}, NO_2, SO_2 and CO_2. Some studies also derived data using aerosol optical depth from MODIS (1km), MISR (275 m) and TROPOMI NO_2 (100 m) (11; 86). A large fraction($\approx$50%) of studies use climate, physical and transport simulation models such CFD, ENVI-met, CMIP and GEOS-Chem to examine pollutant transport, deposition and ventilation under varying urban morphological configurations. Especially for detailed small scale studies, the atmospheric transport, dispersion of pollutants, building configurations and street canyon geometry are easier to study through

simulation models (87; 88).

Wildfire detection and characterization are typically done using medium and coarse spatial resolution satellite fire products such as MODIS burned-area and active-fire product (250 m–1 km), VIIRS active-fire product (375 m) and Sentinel-2 burn-severity and burned-area composites (10–20 m) (67; 89; 90). These are often complemented by fire-weather index inputs from ERA5 reanalysis and NOAA wind and humidity fields (28; 91). At small scales, fire-spread dynamics are frequently modeled using cellular automata, FireSTS and FlamMap simulations (92). The WUI delineation and related medium-resolution urban-form indicators are largely extracted from Sentinel-1/2 and Landsat 8 (13; 89), while high-resolution morphology is mapped using orthorectified aerial photographs (0.2–0.5 m), Google Earth and Bing Maps (0.3–1 m) or drone images (90; 93).

Drought conditions in the selected evidence base are mainly characterized using satellite-derived medium to coarse-resolution products such as MODIS potential evapotranspiration (PET), evapotranspiration (ET), NDVI (250 m–1 km), LST (1 km) and albedo, complemented by AVHRR NDVI time series for long-term drought analysis (50; 71; 72). A large fraction of studies explored drought–urbanization interaction using CMIP5/CMIP6, CESM and WRF simulations (94; 95; 96). The required precipitation and climate forcing are obtained from GPCC (27km), ERA5/ERA5-Land (11km) and national station networks, while hydrological stress and water scarcity are assessed using global water models, catchment-scale water stress indices (WSI) and large-scale urban drought datasets at 100 km resolution (46; 94; 96).

Overall, hazards that can be directly observed from satellites are more strongly associated with remote sensing, whereas hazards governed by subsurface or flow dynamics are predominantly represented through modeling frameworks (Figure 7).

4.2.3 Hazard-Specific Methods

Methods vary in parallel with data regimes 8. Across hazards, empirical analysis is the most commonly used method, which includes the use of regression, correlation, clustering, dimension reduction (10; 97; 98; 99) or basic machine-learning techniques such as gradient boosting and SHAP-based interpretation to capture nonlinear relationships between urban morphology and climate hazards (100; 101; 102). The use of numeric and physical modeling are spread across hazards, which simulate environmental processes through microclimate models, energy balance and radiation schemes, computational fluid dynamics, or building and neighborhood scale physical representations used to examine ventilation, heat transfer, or flood hydraulics (68; 103). However, climate and atmospheric modeling and attribution methods that employ global and regional climate models, reanalysis products and event attribution frameworks are mainly used to study the relationship between landcover types and droughts (96).

Heat-wave and air-quality studies primarily use empirical approaches, reflecting the strong availability of temperature and pollutant monitoring data (11; 98; 104; 105). Air-quality research additionally shows substantial use of physical modeling such as CFD-based simulations, which is essential for representing dispersion processes in street canyons and other complex urban geometries (74; 106; 107). Machine learning appears as a secondary tool in both domains, complementing observational analyses (59; 63; 73; 108). Flood studies show the clearest methodological concentration, dominated by hydrodynamic and process-based models, such as the TELEMAC-2D hydrodynamic model and SHETRAN hydrological model, that incorporate topography, built form and drainage systems (52; 68; 80). Empirical and ML methods play a supporting role, especially for flood susceptibility and classification tasks (55; 102; 109). Landslide studies combine empirical susceptibility analysis with physical slope stability models (CHASM and HRLDAS) and InSAR analysis, although the focus remains case-specific (57; 70; 110). Wildfire studies in urban and WUI settings remain strongly empirical, focused on mapping exposure and settlement patterns rather than applying fire behavior modeling or climate-linked projections (67; 89; 90; 93). Drought studies are, however, characterized by a combination of empirical analysis and climate and atmospheric modeling, with a substantial share of studies drawing on CMIP based climate simulations, reanalysis products and derived hydroclimatic metrics to assess water stress and drought conditions. These approaches emphasize large-scale climate forcing and land–atmosphere interactions rather than neighborhood scale process representation (96; 111; 112).

Overall, Landslide research relies primarily on physical modeling, such as CHASM, HRLDAS (70; 113),

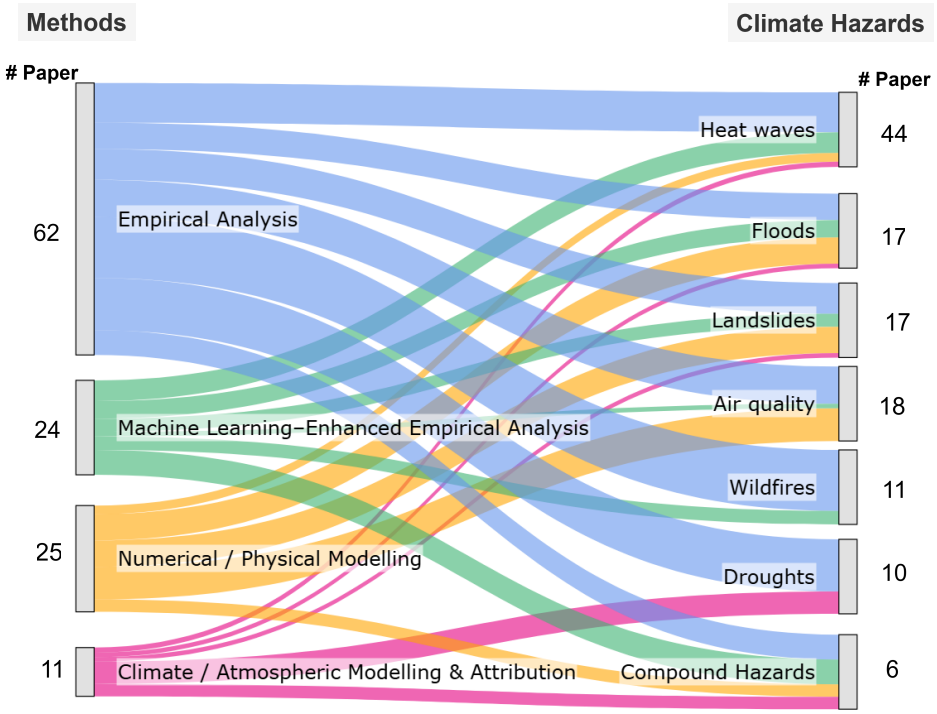

Fig 8. Distribution of Methodological Approaches Across Hazards. Empirical and ML-enhanced methods together dominate the distribution, followed by numerical modeling.

whereas flood studies use a combination of machine-learning empirical analysis (52), hydrodynamic and process-based models, such as TELEMAC-2D, SHETRAN and CFD models (54; 68). Similarly, air quality studies use empirical analysis and numerical modeling of pollutant dispersion.

4.2.4 Morphological Representation Patterns Across Hazards

Variation is equally evident in how urban morphology is represented. No single morphological representation is uniformly applied across hazards (Figure 9). Heat-related studies exhibit the broad diversity of morphological representations, with studies using 2D, 3D building indicators as well as LCZ classifications. Landslide studies frequently use both 2D and 3D building indicators but rarely employ LCZ typologies. Flood and wildfire studies rely predominantly on 2D building indicators, particularly density and building coverage ratio. Air-quality research balances 2D and 3D measures, reflecting the importance of street-canyon ventilation. Compound hazards are rarely studied and mainly rely on 2D building indicators. These patterns indicate that hazard domains differ in the dimensional emphasis placed on urban form, as some domains integrate detailed 3D geometry while others rely primarily on surface-based metrics. Additionally, the integration of urban morphology into hazard analysis is more consolidated and systematically developed in some hazard domains than in others.

4.2.5 Urban Morphology & Climate Hazard Dynamics

Across the literature, urban morphology is treated as a structural driver of hazard variability, with measurable attributes of the built environment used directly as explanatory variables rather than background context. Figure 10 demonstrates that hazards draw on different combinations of morphology indicators: some use overlapping measures, while others rely on hazard-specific metrics, and no single representation of urban form is applied consistently. Urban heat studies, in particular, use a broader range of 2D and 3D indicators, whereas other hazards rely on a more limited subset. These patterns indicate that urban

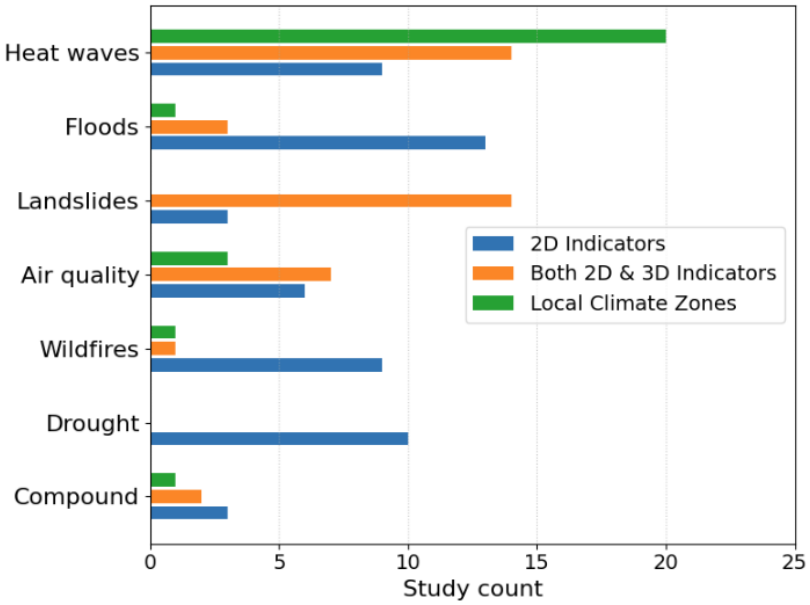

Fig 9. Comparative Use of Urban Morphology Representations Across Hazards. The urban morphologies are represented by 2D/3D building indicators (14) and Local Climate Zones (LCZ) (12). These patterns indicate that different hazards emphasize distinct aspects of urban form.

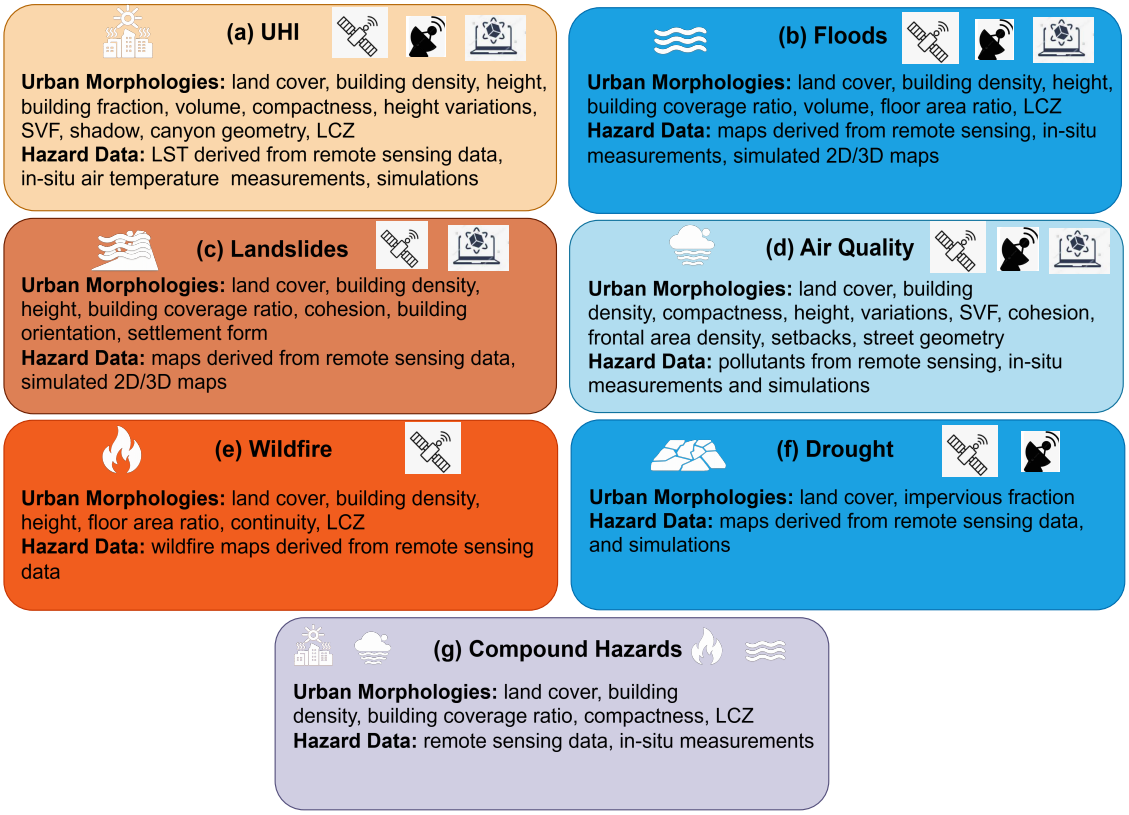

Fig 10. Summary of urban morphologies and climate hazard data used in the reviewed literature.

morphology influences hazards through shared physical processes, but its analytical representation remains fragmented across domains. The following subsections examine each hazard individually, detailing how specific indicators align with underlying mechanisms and where explanatory gaps persist.

Urban Heat Island & Urban Morphology

Across the reviewed studies, a consistent pattern emerges: urban morphology fundamentally structures how heat is generated, stored and redistributed within cities, but the contribution of morphology depends on the type of indicator used.

Two-dimensional descriptors such as building coverage ratio, density, land cover composition and the spatial arrangement of built-up areas, explain broad patterns of surface urban heat islands. Higher imperviousness and compactness increase surface temperatures by enhancing heat absorption and limiting cooling through soil moisture and evaporation, whereas high vegetation fraction and more favorable spatial configuration enhance evapotranspiration, improve soil moisture retention and reduce surface temperatures, helping to moderate heat accumulation across urban areas (26; 27; 100; 114). These 2D indicators are therefore effective in identifying large-scale thermal patterns within cities.

Three-dimensional structure, captured through indicators such as variations in building height, sky-view factor, volumetric density, floor area ratio, and canyon geometry, adds a crucial layer. These 3D morphological indicators determine micro-scale thermal behavior by shaping shading, wind speed, direction, radiative trapping and ventilation (14; 48). Dense, tall configurations tend to intensify night-time UHIs by restricting long-wave cooling (10; 115), while height diversity and optimized canyon geometry can improve daytime thermal comfort (56). Studies comparing surface and canopy UHI (64) show that 3D structure explains discrepancies between surface-level thermal patterns and air-temperature fields, which 2D indicators alone cannot resolve. Moreover, even for heat stress, where the commonly used satellite LST provides rooftop or tree-top temperature, considering 3D urban geometry plays a key role.

The LCZ framework embeds both 2D and 3D characteristics into discrete classes with predictable thermal signatures, providing a useful organizing structure across multiple studies (12). Built-up LCZs consistently exhibit stronger heat-island effects than natural LCZs. Among building types, mid-rise zones (LCZ 2,5,8) often have higher heat-island intensities than low-rise (LCZ 3,6,9) and high-rise building zones (LCZ 1,4,7). Compact configurations (LCZ 1–3) show higher UHI values than open(LCZ 4–6) and spare building configurations (LCZ 7–9). More importantly, compact high-rise buildings are often ranked as coolest during the day due to shading and they are also the hottest during nighttime measurements due to the heat trap effect and reduced airflow caused by tall buildings (63; 116).

Taken together, these findings show that while 2D indicators effectively capture city and regional scale surface heat patterns, 3D morphology and LCZ classifications are essential for explaining neighbourhood scale thermal processes, diurnal contrasts and human-relevant heat exposure within complex urban environments.

Urban Floods & Urban Morphology

Urban flooding is consistently shaped by 2D urban morphology such as impervious surface fraction, building density, coverage ratio and spatial layout. Evidence from multiple river basins and metropolitan regions demonstrates that increasing urbanized and impervious surfaces accelerates runoff, reduces infiltration capacity, intensifies flood peaks and shortens hydrological response times (117; 118; 119). At neighborhood scales, building spacing, block structure and street networks strongly influence where water accumulates during floods. Closely spaced buildings and poorly connected streets tend to trap water, while more open layouts allow runoff to spread or drain more efficiently. As a result, local urban form explains why some streets or blocks repeatedly flood while nearby areas remain relatively dry, even under the same rainfall conditions (79; 102).

Flood behavior is also affected by 3D morphology, especially metrics such as building height distribution, floor area ratio, mean building volume and the standard deviation of building volume, which influence floodwater movement by altering flow constriction, storage potential and hydraulic complexity (102). Higher variability in building volume acts as a flow inhibitor, increasing turbulence and redistributing flood depths, while factors such as under-building openness, setbacks and elevated or “lift-up” architectural forms significantly modify local flood velocities and directions (54; 55). These effects are strongly conditioned by

terrain, with slope and ground elevation governing runoff speed and the formation of waterlogging zones, particularly in low-lying areas with dense or informal settlements (120). Studies using Local Climate Zone (LCZ) classifications show that groups of urban form types with similar building density and surface characteristics also exhibit similar flood behavior, helping to explain differences in flood hazard and vulnerability across cities (121). Hydrodynamic analyses further confirm that features such as building openness and layout symmetry influence flood depth and water distribution at the neighborhood scale (51).

Overall, flood-related studies rely mainly on 2D building indicators, with a smaller number of 3D indicators providing additional insight. Building density, imperviousness, mean building volume, street layout, and slope consistently emerge as the most influential morphological factors shaping urban flood risk.

Landslides & Urban Morphology

Rapid urbanization is driving cities to expand into and around mountainous terrain, where steep slopes and unstable ground amplify hazards. In regions such as Nepal, India and China, the pace of expansion often exceeds the capacity of planning and regulatory frameworks, resulting in development on highly sensitive hill slopes. Landslides in and around such urban areas emerge from the combined effects of anthropogenic slope modification, pre-existing geomorphic instability and extreme rainfall (113).

Urban morphology modifies slope stability through cut-and-fill excavation, terracing, undercutting and the construction of road networks, all of which alter natural slope geometry and drainage pathways (110; 122). Structural loading from multi-story buildings further increases driving forces on slopes, while inadequate drainage and construction waste accumulation elevate pore-water pressures (69; 123). 2D building configuration also affects physical vulnerability: orientation and aspect ratio control how loads are transferred downslope, with wider structures aligned parallel to slope direction exhibiting lower failure potential (124). Increased building density intensifies terrain modification, alters drainage and adds structural load, collectively increasing instability (70). Vegetation patterns introduce additional morphological controls. Deep root systems enhance soil cohesion and shear strength, while canopy interception reduces effective rainfall and runoff, collectively lowering slope-failure potential (125). Geometrical (slope angle and the thickness of the first layer of residual soil) and soil properties are the predisposing factors that most dominate the slope stability response (126). In underdeveloped tropical cities, settlements with informal housing practices such as unregulated deforestation and household water drainage trigger landslides and such communities bear a disproportionate share of fatalities (69; 127).

Overall, landslide studies are dominated by the combination of only a few 2D and 3D indicators, consistently identifying building density, height or loading effects and slope-oriented configuration as the dominant factors influencing urban slope stability.

Air Quality & Urban Morphology

Urban morphology shapes both the generation of urban air pollution and the dispersion processes that determine exposure. At the city scale, 2D indicators of urban structure such as density, compactness, land-use mix, block size and road-network intensity are consistently associated with elevated concentrations of PM2.5, PM10 and NOx. These relationships primarily reflect the spatial concentration of emission sources (especially traffic and energy use), increased imperviousness, and modifications to background ventilation and mixing conditions that regulate the dilution of pollutants within the urban boundary layer (104; 128; 129). These relationships interact with large-scale atmospheric stability: regional stagnation and shifts in circulation can suppress vertical and horizontal exchange, thereby amplifying the ventilation constraints imposed by dense urban forms, particularly in rapidly urbanizing regions. Evidence indicates that cities with larger artificial surface areas tend to exhibit higher NO2 and PM10 concentrations, while densely populated urban systems are more strongly associated with elevated SO2 levels, reflecting differences in dominant emission sources and urban energy structures (128).

At neighborhood and street-canyon scales, 3D morphology indicators such as aspect ratio, building height, height variability, frontal area density, horizontal setback and canyon orientation are important to determine flow structure, pollutant retention and the strength of recirculation cells. Deep, narrow, and enclosed street canyons exhibit reduced ventilation efficiency, leading to pollutant accumulation and prolonged residence time. In contrast, urban configurations with height variability, staggered layouts and permeable fronts

promote stronger mixing and more frequent exchange between canyon air and the atmosphere above, which improves ventilation and leads to lower pollutant concentrations at the pedestrian level. Horizontal building setbacks modify airflow in street canyons by opening up the street space and reducing stagnant circulation. As a result, polluted air can disperse more easily along and across the street, while cleaner air from above the buildings can more readily enter the canyon and carry pollutants upward and away. Setbacks on the windward side are therefore particularly effective at reducing pollution levels in high-rise streets. (23; 107; 130)

Green infrastructure exerts strongly morphology-dependent effects on air quality. Trees, hedges, and vegetative barriers can enhance pollutant dispersion by generating small-scale turbulence and promoting mixing, but they may also obstruct airflow and intensify pollutant trapping when placed in deep or poorly ventilated canyons. The net effect depends on canyon geometry, vegetation porosity, canopy height, and placement relative to dominant flow paths (75; 88; 131). These findings indicate that air pollution patterns are shaped by both 2D and 3D urban morphology, jointly regulating ventilation efficiency and the accumulation or dispersion of pollutants in urban areas.

Wildfires & Urban Morphology

Wildfire risk in urban areas is strongly shaped by the spatial form of development at the wildland–urban interface (WUI), where settlements overlap with flammable vegetation. Literature consistently shows that 2D urban morphology indicators such as housing density, settlement extent and the degree of contact with wildland fuels are the main drivers of human exposure to wildfire. Rapid expansion of low-density development into fire-prone landscapes has therefore markedly increased the number of homes and populations exposed to wildfire in the United States and globally (13; 89).

At the parcel and neighborhood scale, building patterns strongly condition structure loss. Sparse housing arrangement, siting on slopes and ridges and proximity to continuous fuels all emerge as significant predictors of building destruction. Studies show that isolated and scattered housing configurations experience higher building loss than clustered developments, despite similar fire weather conditions. This pattern arises because sparse buildings are often surrounded by continuous vegetation, which allows fire to spread more easily and exposes structures to direct flames and intense heat. In contrast, more compact development tends to fragment vegetated fuels, reduce local fire intensity, and concentrate firefighting resources, lowering the probability of individual structure loss (132; 133).

Local terrain further shapes wildfire impacts by interacting with settlement patterns. Buildings located on slopes or ridges are more vulnerable because fires move faster uphill, heating and drying vegetation ahead of the flame front and increasing fire intensity. These terrain effects are especially strong where low-density housing is built along ridge lines or within steep, fuel-rich landscapes, increasing both exposure and potential damage (134). The 3D urban morphology plays a secondary but important role at the micro scale: building height and slope position influence structure-to-structure ignition, ember trapping and evacuation safety, particularly in steep terrain and irregular street networks. Taller or more exposed buildings are more likely to intercept wind-blown embers, increasing the risk of ignition, particularly in steep areas with irregular street layouts (135).

Overall, wildfire risk in urban areas is most strongly correlated with 2D settlement patterns at the WUI, where housing density, spatial configurations and continuity with flammable vegetation dominate exposure and loss, while 3D features primarily modulate local fire behavior and vulnerability rather than regional risk.

Droughts & Urban Morphology

Urban morphology in the drought literature is mainly included through 2D indicators of urbanization, such as built-up extent, impervious cover, land use, vegetation type and population density, rather than through 3D geometry or LCZ classes. Multiple studies show that urban land cover reduces evapotranspiration, increases heat and raises vapor pressure deficit, which strengthens atmospheric dryness, soil moisture stress relevant for drought processes (136). High-resolution remote sensing analyses confirm that the expansion of built surfaces increases the severity and spatial fragmentation of meteorological drought inside cities (137),

while drought-driven vegetation stress interacts with neighborhood land cover patterns to elevate heat exposure in low canopy districts (138).

Climate modeling simulations show that urbanization suppresses light rainfall and intensifies extreme drought conditions in many global cities (112). Compound-event studies further show that the combined effects of climate change and urban expansion increase the frequency of hot–dry extremes, particularly in rapidly growing urban regions (95) with high impervious surface and low albedo. In parallel, water scarcity studies link urban morphology to drought impacts primarily through demand-side mechanisms. Urban expansion and population growth increase water withdrawals while reducing local recharge, transforming meteorological drought into urban water scarcity (136).

Hydroclimatic reconstructions and attribution studies provide essential context but do not include detailed representations of urban form. They distinguish urban from rural stations or describe general urbanization levels without analyzing the internal configuration of the built environment (137; 139). Across the full set of studies, the link between urban morphology and drought is therefore mediated through urban land cover change, imperviousness, albedo and other planimetric proxies for water stress, which affects evapotranspiration, rainfall suppression, atmospheric dryness and water demand.

Compound Hazards & Urban Morphology

Studies examining concurrent hot and dry extremes and urbanization connected shifts in rainfall and drought primarily link urban impacts to the intensity of urbanization rather than explicit urban form. Compound dry-hot extremes are shown to be amplified by urban development through urban canopy processes, increasing the frequency and persistence of these events beyond greenhouse-gas warming alone (95). Similarly, studies on rainfall asymmetry and drought demonstrate that higher urbanization levels, represented by impervious surface fraction, are associated with intensified heavy rainfall, suppressed light rainfall and more severe drought indicators (50). Across this group, urban morphology is represented mainly through land-cover proxies, despite the acknowledged role of ventilation, heat storage and surface-atmosphere interactions that are inherently 3D.

A clearer morphological signal emerges in hydro-geomorphic compound hazards, particularly wildfire-rainfall-landslide and flood-wildfire interactions. In these studies, wildfires act as a predisposing factor while rainfall functions as the triggering mechanism, with susceptibility strongly governed by terrain variables such as slope, elevation, curvature and wetness indices (140). In multi-hazard flood and wildfire assessments, topography and land use structure the spatial separation and overlap of hazard susceptibility, while building data are used to quantify exposure rather than to modify hazard processes (53). One large-scale study explicitly examining compound natural risks further identifies density, compactness, openness, land-use mix, proximity to roads, slope and greenness as statistically significant factors influencing compound risk patterns, indicating that urban morphology can act as a modifier of multi-hazard risk when explicitly modeled (141). Overall, while compound hazards are increasingly documented across climatic and geomorphic domains, urban morphology is most often simplified to land cover or terrain, with limited integration of structured urban form indicators. The key research gap lies in the systematic incorporation of 3D urban forms and LCZ-based frameworks into compound hazard analysis.

5 Research Gaps

Despite growing recognition of the role of urban morphology in shaping climate hazards, substantial limitations persist in how this relationship is studied, represented and generalized. These limitations arise from multiple sources, including constraints in data availability, resolution and representation, methodological choices that privilege single hazards or specific spatial scales, and structural biases in geographic coverage and urban contexts. Together, they restrict the ability to synthesize findings across hazards and cities and to translate process-level understanding into robust, transferable insight. Clarifying these limitations provides a necessary foundation for identifying priorities for future morphology-aware research and for improving the physical basis of urban climate hazard assessment.

5.1 Topical and Hazard-Specific Gaps

Urban heat stress research relies heavily on satellite-based land surface temperature; however, LST is a poor surrogate for air temperature, especially for summer daytime and under heat stress conditions, when their relationship becomes non-linear (142; 143). Moreover, despite urban heat island (UHI) being predominantly a nighttime phenomenon, much of the literature remains strongly biased toward daytime conditions, with limited systematic analysis of nighttime UHI intensity and diurnal contrasts across different urban forms (78). Compact LCZ classes, particularly high-rise configurations, exhibit lower daytime surface temperatures due to shading while sustaining elevated nighttime temperatures because of low ventilation and trapped heat, yet these contrasting dynamics are rarely examined in a unified framework (62). This limitation is consequential, as compound day-night heat extremes are increasingly more harmful to human health than isolated daytime or nighttime events (47). Moreover, the predominant reliance on satellite-derived land surface temperature limits interpretation, as it reflects roof or canopy conditions rather than near-surface thermal exposure experienced by humans (142; 143; 144).

The literature is skewed towards urban heat, as 36% of the reviewed literature focuses on heat-related hazards (Figure 5). Compared to heat, systematic multi-city analyses of WUI morphology and wildfire risk remain scarce, despite widespread global exposure (145). Urban landslide research is likewise concentrated in a handful of mountainous countries and often ignores 3D urban form (e.g., retaining walls, cut-and-fill terraces, underground structures), limiting understanding of how urban form modifies slope stability and cascading risks (123; 146). Many urban flood studies neglect the role of urban drainage systems, complex slope directionality, and flow obstruction by dense buildings, leading to incomplete characterization of runoff and inundation patterns, particularly in high-density urban areas (68; 102; 109). Heat studies tend to explore a wider range of urban form metrics, while other hazards are often analyzed using a narrow set of variables. As a result, knowledge remains uneven across hazard domains.

Across reviewed literature, only a few studies adopt a compound-hazard perspective (see study count in Figure 7), most often combining heatwaves with air pollution or wildfire with air pollution. This limits understanding of how one hazard can influence another. For example, wildfires can increase landslide risk by removing vegetation, while wildfire and heat can together worsen air pollution by altering chemical processes and airflow (75; 140). In this way, one event can precondition urban landscapes for subsequent hazards, creating cascading risks that are not captured by single-hazard studies. This continued reliance on single-hazard approaches, therefore, limits understanding of how urban form shapes risk under increasingly complex climate extremes.

5.2 Geographic and City-Type Gaps

Our review shows that fast-growing cities in the Global South, as well as small- to medium-sized cities worldwide, are systematically underrepresented in urban morphology-hazard research, despite experiencing rapid land use change, population growth and increasing climate exposure. Existing studies are concentrated in a small number of regions, particularly East Asia and Europe, while rapidly urbanizing areas in Africa, Latin America and other parts of the Global South remain underrepresented, despite experiencing increasing climate exposure (Figure 5). This imbalance is critical because urban form varies widely across regions, reflecting differences in planning systems, building practices and socio-economic conditions. As a result, urban morphology–hazard relationship findings derived from well-studied cities may not apply to other contexts.

Small and medium-sized cities are also largely absent from the literature, despite their growing share of global urbanization. Informal settlements are especially neglected, even though they often face the highest exposure to floods, landslides and heat (69; 120; 127). These areas are typically characterized by compact, low-rise built forms (LCZ 3), which have been consistently associated with high urban heat intensity (147), yet their specific form–hazard relationships remain poorly understood. This limits the ability to design effective adaptation strategies where they are most needed.

5.3 Data and Methodological Gaps

A major constraint in urban morphology and hazard research stems from limited availability of observational data suitable for large-scale three-dimensional and temporal analyses. While multi-temporal global built-up products such as the Global Human Settlement Layer (GHSL), World Settlement Footprint (WSF) Evolution and Global Artificial Impervious Area (GAIA) have enabled systematic analyses of long-term settlement dynamics at regional to global scales(66; 148; 149), they do not provide detailed building footprint information necessary for fine-scale morphology assessment. Consequently, a large share of existing studies rely on simplified surface indicators, such as land cover (150; 151; 152; 153). More recently, WSF-3D (154) and GHSL-Built-H R2023A (155) have extended these global frameworks by adding building height information, thereby providing the first systematic 3D representations of the built environment at global scale. However, their relatively coarse spatial resolution remains insufficient to characterize neighborhood-scale variations in building height, spacing, canyon geometry, and vegetation structure that govern microclimatic processes, flood routing, slope stability, fire spread, and pollutant dispersion.

Only in the last few years have large-scale building footprint datasets such as the Microsoft Global Building Footprints (156), GlobalBuildingAtlas (LOD1) (157) and Google Open Buildings 2.5D (158) become available, offering unprecedented spatial detail and more realistic 3D representation via building footprints with partial height information. Despite their potential, these products are still predominantly single-epoch, and height coverage remains incomplete (e.g. Google Open Buildings 2.5D focuses largely on the Global South, and Microsoft heights are only available for selected regions). As a result, truly harmonized, multi-temporal analyses of evolving 3D urban form remain largely challenging at regional to global scales.

These data constraints are reflected in the inconsistent use and reporting of morphology indicators across the literature. Two-dimensional, three-dimensional and LCZ-based metrics are applied with limited standardization in definitions, thresholds and spatial aggregation, complicating comparison, synthesis, and meta-analysis across studies (116; 159). At city and national scales, assessments often rely on coarse proxies, such as LCZ classifications at 100 m resolution or simplified height and volume metrics, while detailed 3D morphology is largely confined to micro-scale case studies. This fragmentation limits the ability to generalize findings or systematically evaluate how urban form influences climate hazards across contexts.

Spatial and temporal limitations are further compounded by disparities in data availability across regions. Comparative studies often concentrate on data-rich regions with well-maintained climate records, infrastructure inventories, and disaster databases. While global building datasets extend morphological coverage, many developing countries lack complementary hazard, impact, and loss datasets, as noted by the United Nations Office for Disaster Risk Reduction (UNDRR) (127; 160). This imbalance constrains cross-city comparison and reduces the transferability of morphology–hazard relationships derived from well-studied cities to rapidly urbanizing regions. As a result, global understanding of how urban form shapes climate hazard risks remains uneven and geographically biased.

Methodological gaps further constrain progress. Many air quality, flooding, landslide and drought studies rely on simulation models applied at small spatial scales (see Figure 7). These models enable controlled testing of urban form and hazard drivers, especially where observational data are limited. However, they often use simplified representations of building geometry, surface connectivity and hazard processes, and do not capture the variability of real extreme events(51; 70; 87). As a result, findings may diverge from observed conditions, particularly in dense or informal areas where urban structure is complex. Scaling such models to regional or multi-city contexts remains computationally demanding and methodologically limited, restricting their ability to capture broader geographic and climatic variation (69; 161).

Together, these data and methodological limitations hinder the development of integrated, multi-hazard urban climate frameworks and constrain rigorous evaluation of adaptation strategies. The absence of harmonized, multi-temporal global 3D urban datasets, combined with continued reliance on coarse climate projections without urban-scale downscaling, remains a fundamental barrier to assessing how evolving urban form will interact with future climate extremes, particularly in rapidly urbanizing regions.

5.4 Limitations of the Review

The restriction to English-language peer-reviewed international publications from three bibliographic databases (Web of Science, Scopus, Google Scholar) may exclude relevant local or un-indexed research,

particularly from rapidly urbanizing regions in Asia, Africa, and Latin America, and may introduce a bias toward studies reporting statistically significant morphology–hazard relationships, as some findings might be less frequently published in selected indexed outlets. Furthermore, the exclusion of pre-2015 literature may have introduced a recency bias in the morphological indicators and data products captured by the coding framework, as older studies may have relied on lower spatial resolution data sources and different analytical methods that are no longer dominant but remain scientifically relevant. These limitations do not invalidate the findings but should be considered when assessing the completeness and transferability of the synthesized evidence. The findings should be interpreted in the light of the defined scope of the selected literature rather than the full breadth of available approaches and findings globally in entire research history.

6 Conclusions and Future Research

Urban form plays a central role in shaping how climate hazards develop and are experienced in cities. Evidence across hazards shows that characteristics such as density, layout, building and street geometry influence heat retention, water flow, air circulation and fire spread etc. Yet understanding of how urban form shapes climate hazards across cities remains uneven. Most of the literature relies on simplified surface indicators, focuses on individual hazards and draws heavily from a limited set of geographical regions. Earth observation data underpin many of these studies but are often applied through a narrow set of variables, while persistent limitations in spatial scale, temporal resolution and three-dimensional detail. As a result, knowledge of how urban form shapes risk is fragmented and not easily transferable across cities.

Recent advances in global urban datasets, multi-source data fusion and AI-based mapping offer new opportunities to address these limitations. The increasing availability of high-resolution building footprints and emerging global three-dimensional urban morphology products provides a foundation for more consistent and transferable analyses of urban form across cities. At the same time, advances in climate modeling, urban-scale downscaling, and data-driven approaches create opportunities to better link morphology to hazard-generating processes rather than relying on descriptive correlations alone. Fully realizing this potential will require a shift toward integrated, multi-hazard and policy-relevant frameworks that explicitly link urban form, climate extremes and adaptation performance. Building on these insights, future research should prioritize the following directions to strengthen the integration of urban morphology into climate risk assessment and urban adaptation:

- Improve the spatial resolution, temporal consistency, and global accessibility of urban morphology data: Recent advances in large-scale 3D building datasets and globally applicable estimation methods provide important opportunities to move beyond coarse 2D proxies and support more consistent neighborhood-, city-, and regional-scale analyses of urban form. The Global Building Atlas (157) demonstrates the potential of high-resolution 3D building information for capturing fine-scale urban morphology, although its reliance on commercial PlanetScope imagery and its availability only in 2019 highlights the need for more open and temporally extended products. Google Open Buildings 2.5D temporal products (158) represent another major step forward by providing building presence, fractional building counts, and building height estimates for the Global South from 2016–2023 using open Sentinel-2 data. Although not yet global, such products point toward the feasibility of open, temporally consistent morphology datasets. In parallel, globally applicable methods for 3D building height estimation using open Sentinel-1 SAR and Sentinel-2 MSI (162; 163; 164), together with emerging open benchmark datasets for multi-modal, multi-temporal, and multi-resolution building height estimation (165), provide a strong foundation for advancing deep-learning models that can be transferred and scaled across diverse geographic regions. Future research should build on these developments to improve the spatial resolution, temporal continuity, openness, and global comparability of urban morphology information for climate-hazard assessment.

- Develop harmonized multi-hazard, multi-city datasets: Progress toward integrated morphology-aware urban climate risk assessment requires the systematic development of harmonized datasets that combine standardized urban morphology typologies, such as Local Climate Zones (LCZs), with observed, modeled, and projected climate-hazard layers. At present, many studies remain

hazard-specific, city-specific, or dependent on locally available datasets, which limits comparability across urban contexts and makes it difficult to synthesize evidence on how urban form shapes compound and cascading climate risks. Harmonized multi-city datasets that integrate morphology indicators with heat, flooding, drought, air pollution, wildfire exposure, and other relevant hazards would enable more consistent cross-city and cross-regional comparisons. They would also support the identification of recurring morphology–hazard relationships, while allowing local deviations to be interpreted in relation to climate zones, development trajectories, socioeconomic conditions, and data availability. Future research should therefore prioritize open, interoperable, and regularly updated benchmark datasets that link 2D and 3D urban form, land cover, vegetation, population exposure, and multi-hazard information across diverse geographic regions. Such datasets would provide a stronger empirical foundation for transferable models, comparative urban climate studies, and morphology-aware adaptation planning at neighborhood, city, and regional scales.

- Advance integrated multi-hazard and process-aware frameworks: Future studies should move beyond single-hazard and correlation-based analyses toward integrated frameworks that explicitly capture interactions among multiple climate hazards, urban environmental processes, and key morphological features, including density, land use, building form, street configuration, impervious surface, and green–blue infrastructure. At present, much of the evidence remains fragmented across individual hazards, such as heat, flooding, drought, air pollution, wildfire, or wind, and often relies on statistical associations that do not fully explain the underlying physical, ecological, and socio-spatial mechanisms. Process-aware frameworks that combine high-resolution urban morphology data, remote sensing observations, in situ measurements, urban climate models, hydrological models, energy-balance approaches, and scenario-based simulations can help reveal how specific urban forms amplify, mitigate, or redistribute climate risks under different environmental conditions. Such approaches are particularly important for understanding compound and cascading risks, where hazards interact across space and time, such as heat–drought, heat–air pollution, flood–infrastructure disruption, or wildfire–smoke–health impacts. Future research should also strengthen comparative multi-city studies, especially in rapidly urbanizing regions where urban expansion, informal growth, infrastructure deficits, and climate exposure often coincide. By linking morphology-aware modeling with adaptation scenarios, these frameworks can support more robust evaluation of interventions such as densification, ventilation corridors, and green–blue infrastructure under present and future climate extremes.

- Expand research in under-represented regions and city types: Expand research in under-represented regions and city types: Future research should place greater emphasis on fast-growing cities in the Global South, as well as small- and medium-sized cities globally, where rapid urbanization, limited infrastructure capacity, high climate exposure, and socioeconomic vulnerability often intersect. Current evidence on urban morphology and climate hazards remains strongly shaped by data-rich, large metropolitan regions, particularly in Europe, North America, and parts of East Asia, while many cities experiencing the most rapid urban transformation remain under-represented. This geographic imbalance limits the generalizability of existing findings and risks overlooking morphology–hazard relationships that are specific to informal settlements, peri-urban expansion, mixed land-use patterns, infrastructure deficits, and locally distinct building materials and urban forms. Expanding research to these contexts is essential for understanding how urban density, street configuration, building form, vegetation, and green–blue infrastructure influence exposure and adaptive capacity under diverse climatic, institutional, and developmental conditions. Future studies should therefore prioritize co-designed research with local institutions, planning agencies, communities, and stakeholders to improve data availability, validate global products, contextualize analytical frameworks, and ensure that findings are relevant for local decision-making. Strengthening research capacity and open data infrastructures in under-represented regions would also support more equitable global evidence synthesis and enable morphology-aware adaptation strategies that are better aligned with local planning needs, resource constraints, and climate-risk priorities.

- Promote open data, reproducible methods, and open platforms: Future research should place stronger emphasis on open data, reproducible analytical workflows, and interoperable evidence platforms to

improve synthesis, comparability, and policy uptake in morphology-aware urban climate research. At present, many studies rely on locally assembled datasets, proprietary morphology indicators, non-standardized hazard layers, or analytical workflows that are not reusable. This limits the ability to compare findings across cities, reproduce results, conduct large-scale meta-analyses, and translate scientific evidence into planning guidance. Greater transparency in the sharing of urban morphology indicators, hazard datasets, model inputs, code, uncertainty estimates, and validation procedures would strengthen the credibility and cumulative value of this research field. Open and standardized workflows would also make it easier to assess how methodological choices, spatial resolution, temporal coverage, and data quality influence reported morphology–hazard relationships. Future efforts should therefore prioritize FAIR data principles, open-source tools, harmonized metadata, benchmark datasets, and reproducible processing pipelines that can be applied across multiple cities, hazards, and climate regions. Developing open, interoperable platforms that integrate 2D and 3D urban form, climate-hazard observations and projections, exposure indicators, and adaptation-relevant metrics would provide an important foundation for cross-city evidence synthesis. Such platforms could support large-scale comparative studies, inform IPCC and other global assessments, and help planning agencies, researchers, and practitioners identify robust morphology-aware strategies for climate-resilient urban development and adaptation.

Acronyms

AVHRR Advanced Very High Resolution Radiometer

CESM Community Earth System Model

CFD Computational Fluid Dynamics

CHASM Combined Hydrology and Stability Model

CMIP Coupled Model Intercomparison Project

CUHI Canopy Urban Heat Island

DEM Digital Elevation Model

ENVI-met Environmental Microclimate Model

ERA5 ECMWF Reanalysis Version 5

ET Evapotranspiration

FSLAM Fast Shallow Landslide Assessment Model

GEOS-Chem Goddard Earth Observing System Chemistry Model

GPM Global Precipitation Measurement

GPCC Global Precipitation Climatology Centre

HRLDAS High-Resolution Land Data Assimilation System

LCZ Local Climate Zone Classification

MODIS Moderate Resolution Imaging Spectroradiometer

NDVI Normalized Difference Vegetation Index

PET Potential Evapotranspiration

SDGSAT Sustainable Development Science Satellite

SHAP SHapley Additive exPlanations

SHETRAN Système Hydrologique Européen TRANsport

SRTM Shuttle Radar Topography Mission

SUHI Surface Urban Heat Island

TELEMAC-2D Two-Dimensional Hydrodynamic Modelling System

TROPOMI TROPOspheric Monitoring Instrument

UHI Urban Heat Island

uDALES Urban-Distributed Atmospheric Large-Eddy Simulation

VIIRS Visible Infrared Imaging Radiometer Suite

WRF Weather Research and Forecasting Model

WSI Wildfire Severity Index

WUI Wildland–Urban Interface

Acknowledgments

This research was supported by the European Space Agency (ESA) Climate Change Initiative through the project MOnitoring urban MOrphology and Nature-Based Solutions (MOMO-NBS CCI, ESA Contract No. 4000148450).

References

1. Neumann B, Vafeidis AT, Zimmermann J, Nicholls RJ. Future coastal population growth and exposure to sea-level rise and coastal flooding-a global assessment. PloS one. 2015;10(3):e0118571.

2. Hauer ME, Evans JM, Mishra DR. Millions projected to be at risk from sea-level rise in the continental United States. Nature Climate Change. 2016;6(7):691-5.

3. Masson-Delmotte V, Zhai P, Pirani A, Connors SL, Péan C, Berger S, et al. Climate change 2021: the physical science basis. Contribution of working group I to the sixth assessment report of the intergovernmental panel on climate change. 2021;2(1):2391.

4. Robinson A, Lehmann J, Barriopedro D, Rahmstorf S, Coumou D. Increasing heat and rainfall extremes now far outside the historical climate. NPJ Climate and Atmospheric Science. 2021;4(1):45.

5. Howe PD, Mildenberger M, Marlon JR, Leiserowitz A. Geographic variation in opinions on climate change at state and local scales in the USA. Nature climate change. 2015;5(6):596-603.

6. Seto KC, Fragkias M, Güneralp B, Reilly MK. A meta-analysis of global urban land expansion. PloS one. 2011;6(8):e23777.

7. Zhao L, Oppenheimer M, Zhu Q, Baldwin JW, Ebi KL, Bou-Zeid E, et al. Interactions between urban heat islands and heat waves. Environmental research letters. 2018;13(3):034003.

8. Jacobson CR. Identification and quantification of the hydrological impacts of imperviousness in urban catchments: A review. Journal of environmental management. 2011;92(6):1438-48.

9. Ng E. Policies and technical guidelines for urban planning of high-density cities–air ventilation assessment (AVA) of Hong Kong. Building and environment. 2009;44(7):1478-88.

10. Li Y, Schubert S, Kropp JP, Rybski D. On the influence of density and morphology on the Urban Heat Island intensity. Nature communications. 2020;11(1):2647. Available from: https://doi.org/10.1038/s41467-020-16461-9. doi:10.1038/s41467-020-16461-9.

11. Iungman T, Khomenko S, Barboza EP, Cirach M, Gonçalves K, Petrone P, et al. The impact of urban configuration types on urban heat islands, air pollution, CO2 emissions, and mortality in Europe: a data science approach. The Lancet Planetary Health. 2024;8(7):e489-505.

12. Stewart ID, Oke TR. Local climate zones for urban temperature studies. Bulletin of the American Meteorological Society. 2012;93(12):1879-900. Available from: https://doi.org/10.1175/BAMS-D-11-00019.1. doi:10.1175/BAMS-D-11-00019.1.

13. Radeloff VC, Helmers DP, Kramer HA, Stewart SI, et al. Rapid growth of the US wildland-urban interface raises wildfire risk. Proceedings of the National Academy of Sciences. 2018;115(13):3314-9. Available from: https://doi.org/10.1073/pnas.1718850115. doi:10.1073/pnas.1718850115.

14. Liu Y, Wang Z, Liu X, Zhang B. Complexity of the relationship between 2D/3D urban morphology and the land surface temperature: a multiscale perspective. Environmental Science and Pollution Research. 2021;28(47):66804-18. Available from: https://doi.org/10.1007/s11356-021-15177-7. doi:10.1007/s11356-021-15177-7.

15. Meerow S, Newell JP, Stults M. Defining urban resilience: A review. Landscape and urban planning. 2016;147:38-49.

16. Zhao L, Oleson K, Bou-Zeid E, et al. Global multi-model projections of local urban climates. Nature Climate Change. 2021;11:152-7. Available from: https://doi.org/10.1038/s41558-020-00958-8. doi:10.1038/s41558-020-00958-8.

17. Willard-Stepan M, Gomez N, Cardille J, Galbraith E, Bennett E. Assessing the exposure of buildings to long-term sea level rise across the Global South. npj Urban Sustainability. 2025;5(1):72.

18. Global Assessment Report on Disaster Risk Reduction 2022 (GAR);. Accessed: 2025-11-30. https://www.undrr.org/gar/gar2022-our-world-risk-gar.

19. Liberati A, Altman DG, Tetzlaff J, Mulrow C, Gøtzsche PC, Ioannidis JP, et al. The PRISMA statement for reporting systematic reviews and meta-analyses of studies that evaluate healthcare interventions: explanation and elaboration. Bmj. 2009;339.

20. Oke TR. Boundary layer climates. 2002.

21. Masson V. Urban surface modeling and the meso-scale impact of cities. Theoretical and applied climatology. 2006;84(1):35-45.

22. Grimmond CSB, Oke TR. Aerodynamic properties of urban areas derived from analysis of surface form. Journal of applied meteorology. 1999;38(9):1262-92.

23. Hang J, Li Y, Sandberg M, Buccolieri R, Sabatino SD. The influence of building height variability on pollutant dispersion and pedestrian ventilation in idealized high-rise urban areas. Building and Environment. 2012. doi:10.1016/J.BUILDENV.2012.03.023.

24. Bruni G, Reinoso R, Van De Giesen N, Clemens F, Ten Veldhuis J. On the sensitivity of urban hydrodynamic modelling to rainfall spatial and temporal resolution. Hydrology and Earth System Sciences. 2015;19(2):691-709.

25. Yin J, Yu D, Yin Z, Liu M, He Q. Evaluating the impact and risk of pluvial flash flood on intra-urban road network: A case study in the city center of Shanghai, China. Journal of Hydrology. 2016. doi:10.1016/J.JHYDROL.2016.03.037.

26. Zhao L, Lee X, Smith RB, Oleson K. Strong contributions of local background climate to urban heat islands. Nature. 2014;511(7508):216-9.

27. Yan W, Zhou J, Wang X, Luo J, Yang F, Wu R. Vegetation resistance to compound drought and heatwave events buffers the spatial shift velocities of vegetation vulnerability. Communications Earth & Environment. 2025;6(1):320.

28. Bowman DM, Kolden CA, Abatzoglou JT, Johnston FH, van der Werf GR, Flannigan M. Vegetation fires in the Anthropocene. Nature Reviews Earth & Environment. 2020;1(10):500-15.

29. Vardoulakis S, Fisher BE, Pericleous K, Gonzalez-Flesca N. Modelling air quality in street canyons: a review. Atmospheric environment. 2003;37(2):155-82.

30. AR5 Climate Change 2014: Impacts, Adaptation, and Vulnerability;. Accessed: 2025-11-30. https://www.ipcc.ch/report/ar5/wg2/.

31. IPCC. Climate Change 2022: Impacts, Adaptation and Vulnerability. 2022. Available from: https://www.ipcc.ch/report/ar6/wg2/.

32. Global assessment report on disaster risk reduction 2019;. Accessed: 2025-11-30. https://www.undrr.org/publication/global-assessment-report-disaster-risk-reduction-2019.

33. Kropf K. The handbook of urban morphology. 2018.

34. Marshall S, Gil J, Kropf K, Tomko M, Figueiredo L. Street network studies: from networks to models and their representations. Networks and Spatial Economics. 2018;18(3):735-49. Available from: https://doi.org/10.1007/s11067-018-9427-9. doi:10.1007/s11067-018-9427-9.

35. Grimmond S. Urbanization and global environmental change: local effects of urban warming. The Geographical Journal. 2007;173(1):83-8. Available from: https://doi.org/10.1111/j.1475-4959.2007.232_3.x. doi:10.1111/j.1475-4959.2007.232$_3$.x.

36. Masson V, Heldens W, Bocher E, Bonhomme M, Bucher B, Burmeister C, et al. City-descriptive input data for urban climate models: Model requirements, data sources and challenges. Urban Climate. 2020;31:100536. Available from: https://doi.org/10.1016/j.uclim.2019.100536. doi:10.1016/j.uclim.2019.100536.

37. Kumar P, Druckman A, Gallagher J, Gatersleben B, Allison S, Eisenman TS, et al. The nexus between air pollution, green infrastructure and human health. Environment International. 2019. doi:10.1016/J.ENVINT.2019.105181.

38. Liang C, Guan M. Effects of urban drainage inlet layout on surface flood dynamics and discharge. Journal of hydrology. 2024;632:130890.

39. Calviño-Cancela M, Amil MLC, García-Martínez ED, Touza J. Interacting effects of topography, vegetation, human activities and wildland-urban interfaces on wildfire ignition risk. Forest Ecology and Management. 2017. doi:10.1016/J.FORECO.2017.04.033.

40. Yang X, Peng LL, Jiang Z, Chen Y, Yao L, He Y, et al. Impact of urban heat island on energy demand in buildings: Local climate zones in Nanjing. Applied Energy. 2020;260:114279.

41. Chandler J, Cumpston M, Li T, Page MJ, Welch V. Cochrane handbook for systematic reviews of interventions. Hoboken: Wiley. 2019;4(1002):14651858. Available from: https://www.cochrane.org/authors/handbooks-and-manuals/handbook/current.

42. Pullin AS, Stewart GB. Guidelines for systematic review in conservation and environmental management. Conservation biology. 2006;20(6):1647-56. Available from: https://doi.org/10.1111/j.1523-1739.2006.00485.x. doi:10.1111/j.1523-1739.2006.00485.x.

43. GAR Special Report 2023: Mapping Resilience for the Sustainable Development Goals;. Accessed: 2025-11-30. https://www.undrr.org/gar/gar2023-special-report.

44. Zscheischler J, Westra S, Van Den Hurk BJ, Seneviratne SI, Ward PJ, Pitman A, et al. Future climate risk from compound events. Nature climate change. 2018;8(6):469-77. Available from: https://doi.org/10.1038/s41558-018-0156-3. doi:10.1038/s41558-018-0156-3.

45. Wang X, Li H, Sodoudi S. The effectiveness of cool and green roofs in mitigating urban heat island and improving human thermal comfort. Building and Environment. 2022. doi:10.1016/J.BUILDENV.2022.109082.

46. Hao L, Sun G, Huang X, Tang R, Jin K, Lai Y, et al. Urbanization alters atmospheric dryness through land evapotranspiration. npj Climate and Atmospheric Science. 2023;6(1):149.

47. Wang J, Chen Y, Liao W, He G, Tett SF, Yan Z, et al. Anthropogenic emissions and urbanization increase risk of compound hot extremes in cities. Nature Climate Change. 2021;11(12):1084-9.

48. Kabisch N, Remahne F, Ilsemann C, Fricke L. The urban heat island under extreme heat conditions: a case study of Hannover, Germany. Scientific Reports. 2023;13(1):23017.

49. Fang C, Wang S, Li G. Changing urban forms and carbon dioxide emissions in China: A case study of 30 provincial capital cities. Applied energy. 2015;158:519-31.

50. Huang S, Gan Y, Zhang X, Chen N, Wang C, Gu X, et al. Urbanization amplified asymmetrical changes of rainfall and exacerbated drought: Analysis over five urban agglomerations in the Yangtze River Basin, China. Earth's Future. 2023;11(2):e2022EF003117.

51. Balaian SK, Sanders BF, Abdolhosseini Qomi MJ. How urban form impacts flooding. Nature Communications. 2024;15(1):6911. Available from: https://doi.org/10.1038/s41467-024-50347-4. doi:10.1038/s41467-024-50347-4.

52. Qin X, Wu Y, Huang H, Yang X, Gao L. Impact of impervious surface spatial morphologies on urban waterlogging: insights from a cascade modeling chain at catchment scale. Sustainable Cities and Society. 2025:106912.

53. Luu C, Forino G, Yorke L, Ha H, Bui QD, Tran HH, et al. Integrating susceptibility maps of multiple hazards and building exposure distribution: a case study of wildfires and floods for the province of Quang Nam, Vietnam. Natural Hazards and Earth System Sciences. 2024;24(12):4385-408.

54. Liu S, Zhu Z, Wu W, Zhang D, Peng D, Pang B. Effects of lift-up building design, building setback, and urban open space on pedestrian danger under the joint effect of floodwater and wind. Urban Climate. 2024. doi:10.1016/J.UCLIM.2024.102215.

55. Huang Y, Lin J, He X, Lin Z, Wu Z, Zhang X. Assessing the scale effect of urban vertical patterns on urban waterlogging: An empirical study in Shenzhen. Environmental Impact Assessment Review. 2024;106:107486.

56. Shareef S, Abu-Hijleh B. The effect of building height diversity on outdoor microclimate conditions in hot climate. A case study of Dubai-UAE. urban climate. 2020. doi:10.1016/J.UCLIM.2020.100611.

57. Maraun D, Knevels R, Mishra AN, Truhetz H, Bevacqua E, Proske H, et al. A severe landslide event in the Alpine foreland under possible future climate and land-use changes. Communications Earth & Environment. 2022;3(1):87.

58. Zhou Z, Chen Y. How urban land expansion alters terrain in mountainous and hilly areas: An empirical study in China. Geography and Sustainability. 2025:100304.

59. Huang Z, Duan L, Xu Y, Yang S, Lin Z, Yue H, et al. Exploring the influence of urban green space and urban morphology on urban heat Islands using street view and satellite imagery. Scientific Reports. 2025;15(1):23759.

60. Rodríguez MC, Dupont-Courtade L, Oueslati W. Air pollution and urban structure linkages: Evidence from European cities. Renewable and Sustainable Energy Reviews. 2016;53:1-9.

61. Zhou B, Rybski D, Kropp JP. The role of city size and urban form in the surface urban heat island. Scientific reports. 2017;7(1):4791.

62. Zhang L, Nikolopoulou M, Guo S, Song D. Impact of LCZs spatial pattern on urban heat island: A case study in Wuhan, China. Building and Environment. 2022;226:109785.

63. Yang J, Wang Y, Xiu C, Xiao X, Xia J, Jin C. Optimizing local climate zones to mitigate urban heat island effect in human settlements. Journal of Cleaner Production. 2020;275:123767.

64. Peng W, Wang R, Duan J, Gao W, Fan Z. Surface and canopy urban heat islands: Does urban morphology result in the spatiotemporal differences? urban climate. 2022. doi:10.1016/J.UCLIM.2022.101136.

65. Han W. Analyzing the scale dependent effect of urban building morphology on land surface temperature using random forest algorithm. Scientific Reports. 2023. doi:10.1038/S41598-023-46437-W.

66. Schug F, Bar-Massada A, Carlson AR, Cox H, Hawbaker TJ, Helmers DP, et al. The global wildland–urban interface. Nature. 2023. doi:10.1038/S41586-023-06320-0.

67. Fernández-García V, Beltrán-Marcos D, Calvo L. Building patterns and fuel features drive wildfire severity in wildland-urban interfaces in Southern Europe. Landscape and Urban Planning. 2023;231:104646.

68. Mei C, Shi H, Liu J, Song T, Wang J, Gao X, et al. Analyzing urban form influence on pluvial flooding via numerical experiments using random slices of actual city data. Journal of Hydrology. 2024;633:130916.

69. Bozzolan E, Holcombe E, Pianosi F, Wagener T. Including informal housing in slope stability analysis–an application to a data-scarce location in the humid tropics. Natural Hazards and Earth System Sciences Discussions. 2020;2020:1-20.

70. Bozzolan E, Holcombe EA, Pianosi F, Marchesini I, Alvioli M, Wagener T. A mechanistic approach to include climate change and unplanned urban sprawl in landslide susceptibility maps. Science of the total environment. 2023;858:159412.

71. Manoli G, Fatichi S, Schläpfer M, Yu K, Crowther TW, Meili N, et al. Magnitude of urban heat islands largely explained by climate and population. Nature. 2019;573(7772):55-60.

72. Wang Z, Li J, Hou J, Zhao K, Wu R, Sun B, et al. Enhanced evapotranspiration induced by vegetation restoration may pose water resource risks under climate change in the Yellow River Basin. Ecological Indicators. 2024;162:112060.

73. Huang C, Hu T, Duan Y, Li Q, Chen N, Wang Q, et al. Effect of urban morphology on air pollution distribution in high-density urban blocks based on mobile monitoring and machine learning. Building and Environment. 2022;219:109173.

74. Augusto B, Lopes D, Rafael S, Coelho MC, Ferreira J. Assessing the impact of different urban morphology scenarios on air pollutant emissions distribution. Science of The Total Environment. 2024;950:175341.

75. Abhijith KV, Kumar P, Gallagher J, McNabola A, Baldauf R, Pilla F, et al. Air pollution abatement performances of green infrastructure in open road and built-up street canyon environments – A review. Atmospheric Environment. 2017. doi:10.1016/J.ATMOSENV.2017.05.014.

76. Bechtel B, Demuzere M, Mills G, Zhan W, Sismanidis P, Small C, et al. SUHI analysis using Local Climate Zones—A comparison of 50 cities. Urban Climate. 2019;28:100451.

77. Li Y, Svenning J, Zhou W, Zhu K, Abrams JF, Lenton TM, et al. Green spaces provide substantial but unequal urban cooling globally. Nature Communications. 2024. doi:10.1038/S41467-024-51355-0.

78. Krayenhoff ES, Moustaoui M, Broadbent AM, Gupta V, Georgescu M. Diurnal interaction between urban expansion, climate change and adaptation in US cities. Nature Climate Change. 2018;8(12):1097-103.

79. Mei C, Liu J, Shi H, Wang H, Wang J, Dong L, et al. Exploring impact of street layout on urban flood risk of people and vehicles under extreme rainfall based on numerical experiments. Science China Technological Sciences. 2023. doi:10.1007/S11431-022-2393-2.

80. Lu X, Xu Z, Li Y, Hu X, Song P, Shi Q. A Micro-Macro Coupled Approach to Assess Urban Road Traffic Flood Risk at the City Scale. Available at SSRN 5266916. 2026.

81. Chen L, Guo Z, Yin K, Shrestha DP, Jin S. The influence of land use and land cover change on landslide susceptibility: a case study in Zhushan Town, Xuan'en County (Hubei, China). Natural hazards and earth system sciences. 2019;19(10):2207-28.

82. Depicker A, Jacobs L, Mboga N, Smets B, Van Rompaey A, Lennert M, et al. Historical dynamics of landslide risk from population and forest-cover changes in the Kivu Rift. Nature Sustainability. 2021;4(11):965-74.

83. He Y, Ding M, Duan Y, Zheng H, Wu J, Feng L. Exploring the dynamic impact of urbanization on landslide susceptibility in Sichuan Province using an explainable XGBoost model. Engineering Geology. 2025:108372.

84. Hürlimann M, Guo Z, Puig-Polo C, Medina V. Impacts of future climate and land cover changes on landslide susceptibility: Regional scale modelling in the Val d'Aran region (Pyrenees, Spain). Landslides. 2022;19(1):99-118.

85. Froude MJ, Petley DN. Global fatal landslide occurrence from 2004 to 2016. Natural Hazards and Earth System Sciences. 2018;18(8):2161-81.

86. Alari A, Ballester J, Milà C, Benmarhnia T, Sofiev M, Uppstu A, et al. Quantifying the short-term mortality effects of wildfire smoke in Europe: a multicountry epidemiological study in 654 contiguous regions. The Lancet Planetary Health. 2025;9(8).

87. Krüger E, Minella F, Rasia F. Impact of urban geometry on outdoor thermal comfort and air quality from field measurements in Curitiba, Brazil. Building and environment. 2011;46(3):621-34.

88. Jeanjean APR, Monks PS, Leigh RJ. Modelling the effectiveness of urban trees and grass on PM 2.5 reduction via dispersion and deposition at a city scale. Atmospheric Environment. 2016. doi:10.1016/J.ATMOSENV.2016.09.033.

89. Schug F, Bar-Massada A, Carlson AR, Cox H, Hawbaker TJ, Helmers D, et al. The global wildland–urban interface. Nature. 2023;621(7977):94-9.

90. Chen B, Wu S, Jin Y, Song Y, Wu C, Venevsky S, et al. Wildfire risk for global wildland–urban interface areas. Nature Sustainability. 2024;7(4):474-84.

91. Jain P, Barber QE, Taylor SW, Whitman E, Castellanos Acuna D, Boulanger Y, et al. Drivers and impacts of the record-breaking 2023 wildfire season in Canada. Nature Communications. 2024;15(1):6764.

92. Ju X, Zhong S, Yue Z, Zhu W. Dynamic Risk Assessment of Wui Fires Based on Knowledge-Driven Approach and Scenario Simulation. Available at SSRN 5232109.

93. Fox D, Carrega P, Ren Y, Caillouet P, Bouillon C, Robert S. How wildfire risk is related to urban planning and Fire Weather Index in SE France (1990–2013). Science of the total environment. 2018;621:120-9.

94. He C, Liu Z, Wu J, Pan X, Fang Z, Li J, et al. Future global urban water scarcity and potential solutions. Nature communications. 2021;12(1):4667.

95. Ghanbari M, Arabi M, Georgescu M, Broadbent AM, et al. The role of climate change and urban development on compound dry-hot extremes across US cities. Nature Communications. 2023;14:3509. Available from: `https://doi.org/10.1038/s41467-023-39205-x`. doi:10.1038/s41467-023-39205-x.

96. Ravinandrasana VP, Franzke CL. The first emergence of unprecedented global water scarcity in the Anthropocene. Nature Communications. 2025;16(1):8281.

97. Zhao Y, Chen Y, Li K. Revealing the impacts of 3D urban morphology on surface temperature considering geometry heterogeneity, component contribution, and scale effect. Sustainable Cities and Society. 2025;119:106093.

98. Yuan M, Song Y, Huang Y, Hong S, Huang L. Exploring the association between urban form and air quality in China. Journal of Planning Education and Research. 2018;38(4):413-26.

99. Iungman T, Khomenko S, Barboza EP, Cirach M, Gonçalves K, Petrone P, et al. The impact of urban configuration types on urban heat islands, air pollution, CO2 emissions, and mortality in Europe: a data science approach. The Lancet Planetary health. 2024. doi:10.1016/S2542-5196(24)00120-7.

100. Huang CJ, Liu P, Ma T, Xue H, Wang P, Li D. Analysis of the impact mechanisms and driving factors of urban spatial morphology on urban heat islands. Scientific Reports. 2025. doi:10.1038/S41598-025-04025-0.

101. Yang J, Li H, Xin J, Yu W, Ren J, Yu H, et al. Investigating the effect of urban form on land surface temperature at block and grid scales based on XGBoost-SHAP. Environmental Modelling amp; Software. 2025. doi:10.1016/J.ENVSOFT.2025.106738.

102. Wang M, Li Y, Yuan H, Zhou S, Wang Y, Ikram RMA, et al. An XGBoost-SHAP approach to quantifying morphological impact on urban flooding susceptibility. Ecological Indicators. 2023;156:111137.

103. Forgiarini APP, de Figueiredo SA, Calliari LJ, Goulart ES, Marques W, Trombetta TB, et al. Quantifying the geomorphologic and urbanization influence on coastal retreat under sea level rise. Estuarine, Coastal and Shelf Science. 2019;230:106437.

104. Liang L, Gong P. Urban and air pollution: a multi-city study of long-term effects of urban landscape patterns on air quality trends. Scientific Reports. 2020. doi:10.1038/S41598-020-74524-9.

105. Calhoun ZD, Willard F, Ge C, Rodriguez C, Bergin M, Carlson D. Estimating the effects of vegetation and increased albedo on the urban heat island effect with spatial causal inference. Scientific Reports. 2024;14(1):540.

106. Yang H, Lam CKC, Lin Y, Chen L, Mattsson M, Sandberg M, et al. Numerical investigations of Re-independence and influence of wall heating on flow characteristics and ventilation in full-scale 2D street canyons. Building and Environment. 2021;189:107510.

107. Li Z, Zhang H, Juan YH, Wen CY, Yang AS. Effects of building setback on thermal comfort and air quality in the street canyon. Building and Environment. 2022;208:108627.

108. Zhou L, Yuan B, Hu F, Wei C, Dang X, Sun D. Understanding the effects of 2D/3D urban morphology on land surface temperature based on local climate zones. Building and Environment. 2022;208:108578.

109. Li Z, Wang Z, Wu L, Huang W, Peng W. Evaluating the effect of building patterns on urban flooding based on a boosted regression tree: A case study of Beijing, China. Hydrological Processes. 2023;37(8):e14932.

110. Dille A, Dewitte O, Handwerger AL, d'Oreye N, Derauw D, Bamulezi GG, et al. Acceleration of a large deep-seated tropical landslide due to urbanization feedbacks. Nature Geoscience. 2022. Available from: https://doi.org/10.1038/s41561-022-01073-3. doi:10.1038/s41561-022-01073-3.

111. Zhang Q, Kong D, Singh VP, Shi P. Response of vegetation to different time-scales drought across China: Spatiotemporal patterns, causes and implications. Global and Planetary Change. 2017;152:1-11.

112. Huang S, Wang S, Gan Y, Wang C, Horton DE, Li C, et al. Widespread global exacerbation of extreme drought induced by urbanization. Nature Cities. 2024;1(9):597-609.

113. Kechebour BE. Relation between stability of slope and the urban density: case study. Procedia Engineering. 2015;114:824-31.

114. Schwaab J, Schwaab J. Sprawl or compactness? How urban form influences urban surface temperatures in Europe. City and Environment Interactions. 2022. doi:10.1016/J.CACINT.2022.100091.

115. Wilson C, Shonk JKP, Bohnenstengel SI, Paschalis A, Reeuwijk Mv. Microscale to neighbourhood scale: Impact of shading on urban climate. Building and Environment. 2025. doi:https://doi.org/10.1016/j.buildenv.2025.112721.

116. Rahmani N, Sharifi A. Urban heat dynamics in Local Climate Zones (LCZs): A systematic review. Building and Environment. 2025;267:112225.

117. Du J, Cheng L, Zhang Q, Yang Y, Xu W. Different Flooding Behaviors Due to Varied Urbanization Levels within River Basin: A Case Study from the Xiang River Basin, China. International Journal of Disaster Risk Science. 2019. doi:10.1007/S13753-018-0195-4.

118. Bae S, Chang H. Urbanization and floods in the Seoul Metropolitan area of South Korea: What old maps tell us. International journal of disaster risk reduction. 2019. doi:10.1016/J.IJDRR.2019.101186.

119. Hodgkins GA, Dudley RW, Archfield SA, Renard B. Effects of climate, regulation, and urbanization on historical flood trends in the United States. Journal of Hydrology. 2019. doi:10.1016/J.JHYDROL.2019.03.102.

120. Kaiser ZA, Akter F. From risk to resilience and sustainability: addressing urban flash floods and waterlogging. Risk Sciences. 2025;1:100011.

121. Tu J, Reimuth A, Garschagen M. Exploring the relationship between urban morphology types and household-level flood vulnerability profiles in Ho Chi Minh City. 2024. doi:10.5194/EGUSPHERE-EGU24-16498.

122. Gariano SL, Guzzetti F. Landslides in a changing climate. Earth-Science Reviews. 2016;162:227-52. Available from: https://doi.org/10.1016/j.earscirev.2016.08.011.

123. Holcombe EA, Beesley ME, Vardanega PJ, Sorbie R. Urbanisation and landslides: hazard drivers and better practices. In: Proceedings of the Institution of Civil Engineers-Civil Engineering. vol. 169. Thomas Telford Ltd; 2016. p. 137-44.

124. Chen Q, Chen L, Gui L, Yin K, Shrestha DP, Du J, et al. Assessment of the physical vulnerability of buildings affected by slow-moving landslides. Natural hazards and earth system sciences. 2020;20(9):2547-65.

125. Sharma A, Sajjad H, Rahaman MH, Saha TK, Bhuyan N, Masroor M, et al. Landslide risk using Geospatial techniques and machine learning: Shimla district of Himachal pradesh, India. Environmental Earth Sciences. 2025;84(18):510.

126. Ullah R, Abdullah R, Kassim A, Yunus NZM, Sendo H. Assessment of residual soil properties for slope stability analysis. GEOMATE Journal. 2021;21(86):72-80.

127. Ozturk U, Bozzolan E, Holcombe EA, Shukla R, Pianosi F, Wagener T. How climate change and unplanned urban sprawl bring more landslides. Nature. 2022;608(7922):262-5.

128. Rodríguez MC, Dupont-Courtade L, Oueslati W. Air pollution and urban structure linkages: Evidence from European cities. Renewable Sustainable Energy Reviews. 2016. doi:10.1016/J.RSER.2015.07.190.

129. Oshrieh R, Valipour E. The Role Of Urban Density And Morphology In The Air Pollution Of Tehran Metropolitan. Journal of Contemporary Urban Affairs. 2019. doi:10.25034/IJCUA.2018.4680.

130. Muniz-Gäal LP, Pezzuto CC, Carvalho MFHd, Mota LTM. Urban geometry and the microclimate of street canyons in tropical climate. Building and Environment. 2020. doi:10.1016/J.BUILDENV.2019.106547.

131. Baldauf R. Roadside vegetation design characteristics that can improve local, near-road air quality. Transportation Research Part D-transport and Environment. 2017. doi:10.1016/J.TRD.2017.03.013.

132. Fox D, Carrega P, Ren Y, Caillouet P, Bouillon C, Robert S. How wildfire risk is related to urban planning and Fire Weather Index in SE France (1990-2013). Science of The Total Environment. 2018. doi:10.1016/J.SCITOTENV.2017.11.174.

133. Fernández-García V, Beltrán-Marcos D, Calvo L, Fernández-García V, Beltrán-Marcos D, Calvo L. Building patterns and fuel features drive wildfire severity in wildland-urban interfaces in Southern Europe. Landscape and Urban Planning. 2023. doi:10.1016/J.LANDURBPLAN.2022.104646.

134. Alexandre PM, Stewart SI, Mockrin MH, Keuler NS, Syphard AD, Bar-Massada A, et al. The relative impacts of vegetation, topography and spatial arrangement on building loss to wildfires in case studies of California and Colorado. Landscape Ecology. 2016. doi:10.1007/S10980-015-0257-6.

135. Aguirre P, León J, González-Mathiesen C, Román R, Penas M, Ogueda A. Modelling the vulnerability of urban settings to wildland–urban interface fires in Chile. Natural Hazards and Earth System Sciences. 2024. doi:10.5194/NHESS-24-1521-2024.

136. Zhang X, Chen N, Sheng H, Ip C, Yang L, Chen Y, et al. Urban drought challenge to 2030 sustainable development goals. Science of the Total Environment. 2019;693:133536.

137. Huang S, Wang S, Chen JM, Wang C, Zhang X, Wu J, et al. Urbanization-induced spatial and temporal patterns of local drought revealed by high-resolution fused remotely sensed datasets. Remote Sensing of Environment. 2024. doi:10.1016/J.RSE.2024.114378.

138. Dong C, Yu Y, Guo J, Lin K, Chen X, Okin GS, et al. Drought-vulnerable vegetation increases exposure of disadvantaged populations to heatwaves under global warming: A case study from Los Angeles. Sustainable cities and society. 2023. doi:10.1016/J.SCS.2023.104488.

139. Williams P, Cook BI, Smerdon JE. Rapid intensification of the emerging southwestern North American megadrought in 2020–2021. Nature Climate Change. 2022. doi:10.1038/S41558-022-01290-Z.

140. Di Napoli M, Marsiglia P, Di Martire D, Ramondini M, Ullo SL, Calcaterra D. Landslide susceptibility assessment of wildfire burnt areas through earth-observation techniques and a machine learning-based approach. Remote Sensing. 2020;12(15):2505.

141. He W, Weng Q. Disparities of urban morphology effects on compound natural risks: a multiscale study across the USA. npj Urban Sustainability. 2025;5(1):39.

142. Naserikia M, Nazarian N, Hart MA, Sismanidis P, Kittner J, Bechtel B. Multi-city analysis of satellite surface temperature compared to crowdsourced air temperature. Environmental Research Letters. 2024;19(12):124063.

143. Briegel F, Pinto JG, Christen A. Is satellite land surface temperature an appropriate proxy for intra-urban variability of daytime heat stress? Remote Sensing of Environment. 2025. doi:10.1016/J.RSE.2025.115045.

144. Zhan W, Bechtel B, Du H, Chakraborty T, Kotthaus S, Krayenhoff ES, et al. Satellite-derived Land Surface Temperatures Strongly Mischaracterise Urban Heat Hazard. arXiv preprint arXiv:250916568. 2025.

145. Syphard AD, Keeley JE, Pfaff AH, Ferschweiler K. Human presence diminishes the importance of climate in driving fire activity across the United States. Proceedings of the National Academy of Sciences. 2017;114(52):13750-5.

146. Finno RJ, Voss Jr FT, Rossow E, Blackburn JT. Evaluating damage potential in buildings affected by excavations. Journal of geotechnical and geoenvironmental engineering. 2005;131(10):1199-210.

147. Yang J, Zhan Y, Xiao X, Xia JC, Sun W, Li X. Investigating the diversity of land surface temperature characteristics in different scale cities based on local climate zones. Urban Climate. 2020;34:100700.

148. Liang L, Gong P. Urban and air pollution: A multi-city study of long-term effects of urban landscape patterns on air quality trends. Scientific Reports. 2020. Available from: https://doi.org/10.1038/s41598-020-74524-9. doi:10.1038/s41598-020-74524-9.

149. Wu S, Jin Y, Song Y, Wu C, Venevsky S, et al. Wildfire risk for global wildland–urban interface areas. Nature Sustainability. 2024. doi:10.1038/S41893-024-01291-0.

150. Jeanjean AP, Monks PS, Leigh RJ. Modelling the effectiveness of urban trees and grass on PM2. 5 reduction via dispersion and deposition at a city scale. Atmospheric Environment. 2016;147:1-10.

151. Li D, Liao W, Rigden AJ, Liu X, Wang D, Malyshev S, et al. Urban heat island: Aerodynamics or imperviousness? Science Advances. 2019;5(4):eaau4299.

152. Hodgkins G, Dudley R, Archfield SA, Renard B. Effects of climate, regulation, and urbanization on historical flood trends in the United States. Journal of Hydrology. 2019;573:697-709.

153. Moazzam MFU, Kim S, Lee BG. Cities in the heat: Unveiling the urbanized impacted surface urban heat island of South Korea's metropolises. Remote Sensing Applications: Society and Environment. 2024;36:101271.

154. Marconcini M, Metz-Marconcini A, Esch T, Gorelick N. Understanding current trends in global urbanisation-the world settlement footprint suite. GI_Forum. 2021.

155. Pesaresi M, Corbane C, Ren C, Edward N. Generalized Vertical Components of built-up areas from global Digital Elevation Models by multi-scale linear regression modelling. Plos one. 2021;16(2):e0244478.

156. Microsoft ML Building Heights;. Accessed: 2024-12-30. https://github.com/microsoft/GlobalMLBuildingFootprints.

157. Zhu XX, Chen S, Zhang F, Shi Y, Wang Y. GlobalBuildingAtlas: an open global and complete dataset of building polygons, heights and LoD1 3D models. Earth System Science Data. 2025;17(12):6647-68. Available from: https://essd.copernicus.org/articles/17/6647/2025/. doi:10.5194/essd-17-6647-2025.

158. Sirko W, Brempong EA, Marcos JT, Annkah A, Korme A, Hassen MA, et al. High-resolution building and road detection from sentinel-2. arXiv preprint arXiv:231011622. 2023.

159. Stuhlmacher M, Georgescu M, Turner II B, Hu Y, Goldblatt R, Gupta S, et al. Are global cities homogenizing? An assessment of urban form and heat island implications. Cities. 2022;126:103705.

160. Aronsson-Storrier M. UN office for disaster risk reduction (2019). YB Int'l Disaster L Online. 2021;2:377.

161. Li Z, Zhang H, Wen CY, Yang AS, Juan YH. Effects of frontal area density on outdoor thermal comfort and air quality. Building and Environment. 2020;180:107028.

162. Yadav R, Nascetti A, Ban Y. How high are we? Large-scale building height estimation at 10 m using Sentinel-1 SAR and Sentinel-2 MSI time series. Remote Sensing of Environment. 2025;318:114556.

163. Cao Y, Weng Q. A deep learning-based super-resolution method for building height estimation at 2.5 m spatial resolution in the Northern Hemisphere. Remote Sensing of Environment. 2024;310:114241.

164. Xu Q, Guan X, Li X, Yang X, Teng Y, Wu H. EL-Mamba: An edge-aware and locally-aggregated Mamba network for building height estimation using Sentinel-1 and Sentinel-2 imagery. International Journal of Applied Earth Observation and Geoinformation. 2026;146:105103.

165. Yadav R, Nascetti A, Ban Y. A Multi-Modal, Multi-Temporal, Multi-Resolution Benchmark Dataset for Building Height Estimation. Scientific Data. 2025.